

Understanding and modeling dense overflows

Sonya Legg

Princeton University

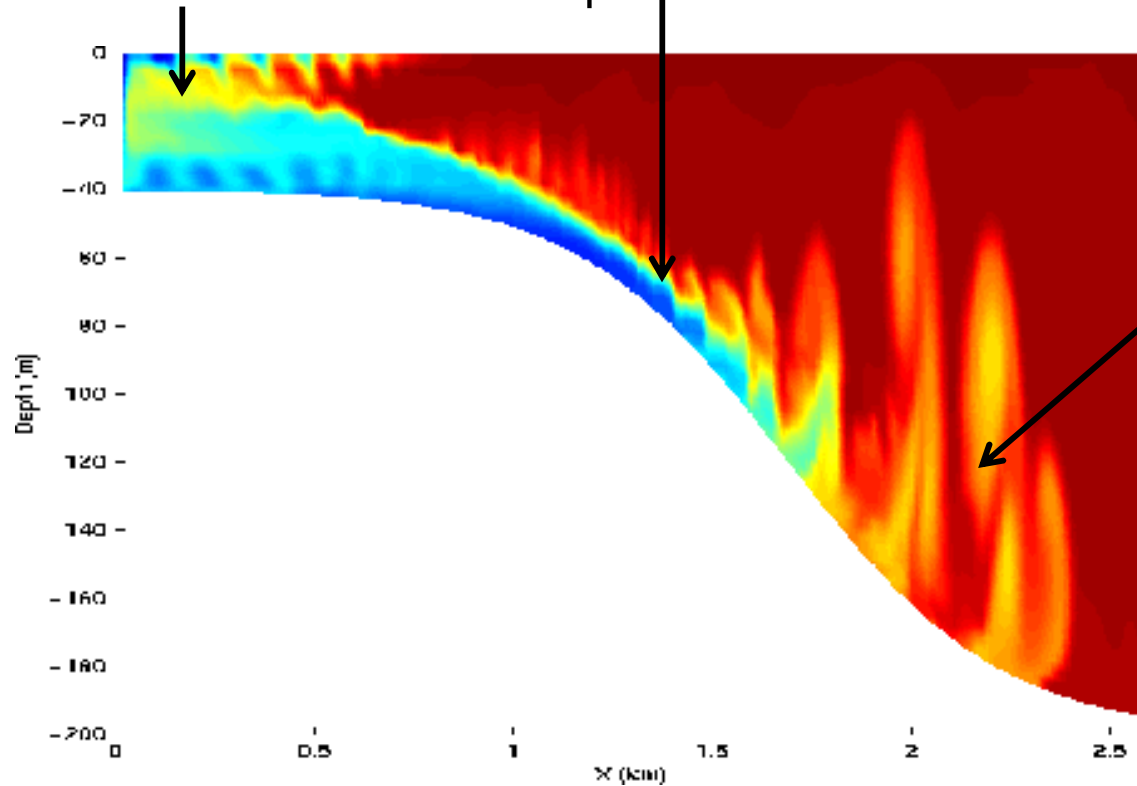
AOMIP/FAMOS school for young
scientists 2012

What is an overflow?

Dense water formation
on shelf or marginal sea

Dense water
accelerates down
slope

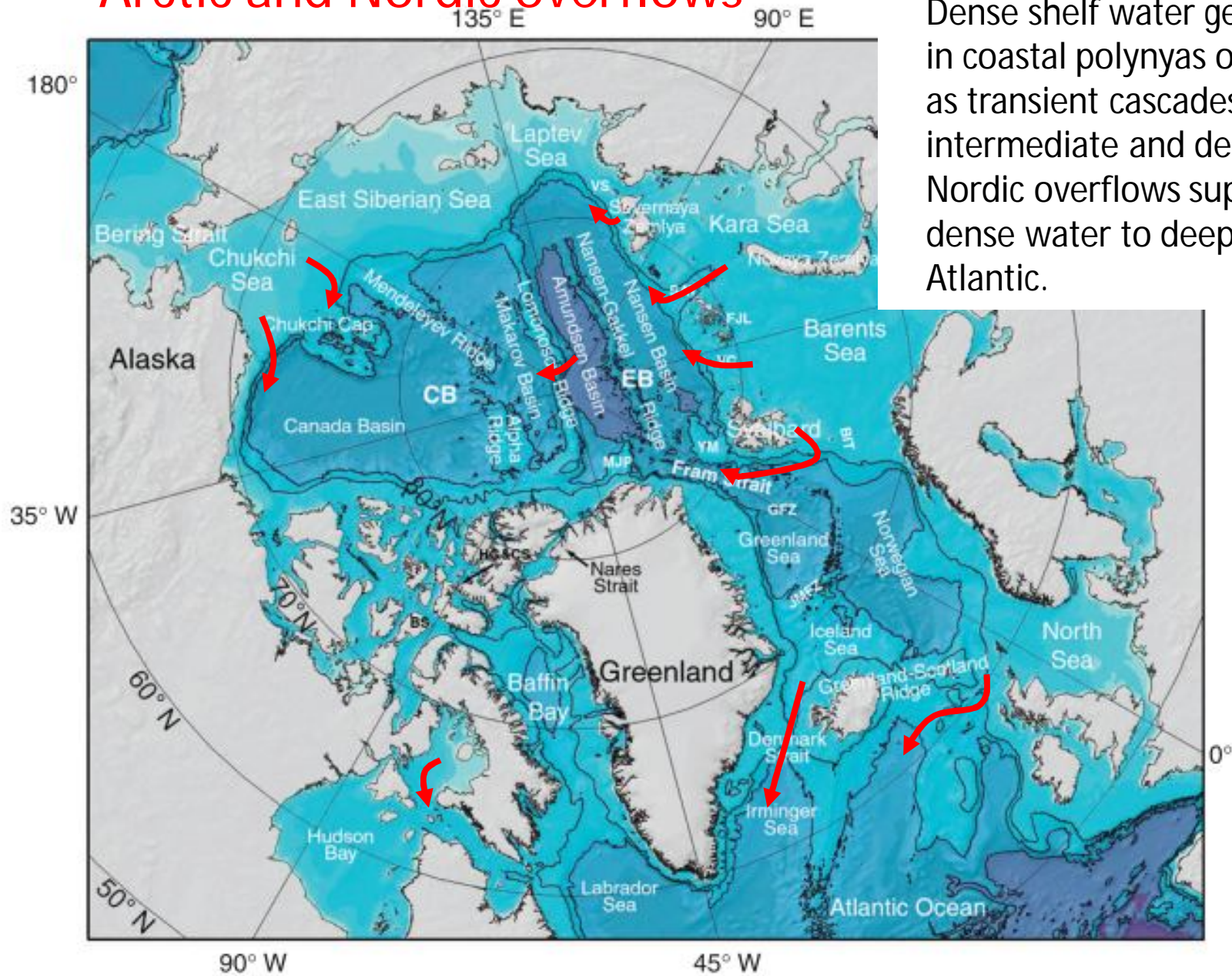
Mixing dilutes
dense water



(Idealized non-rotating MITgcm simulation)

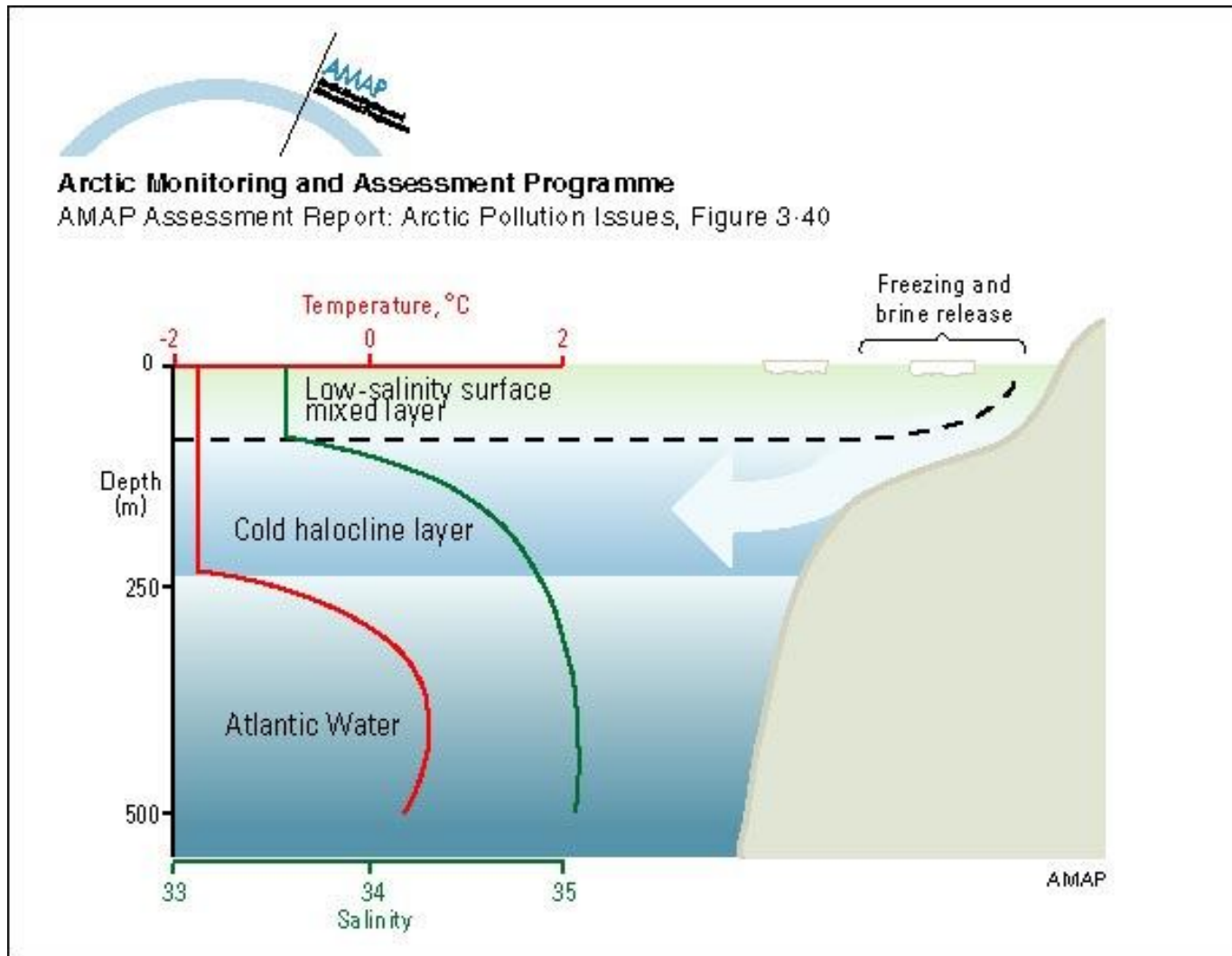
Arctic and Nordic overflows

Dense shelf water generated in coastal polynyas overflows as transient cascades to fill intermediate and deep Arctic. Nordic overflows supply dense water to deep North Atlantic.



(Bathymetric map from Rudels, 2009)

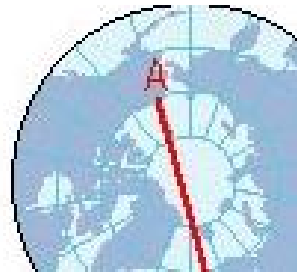
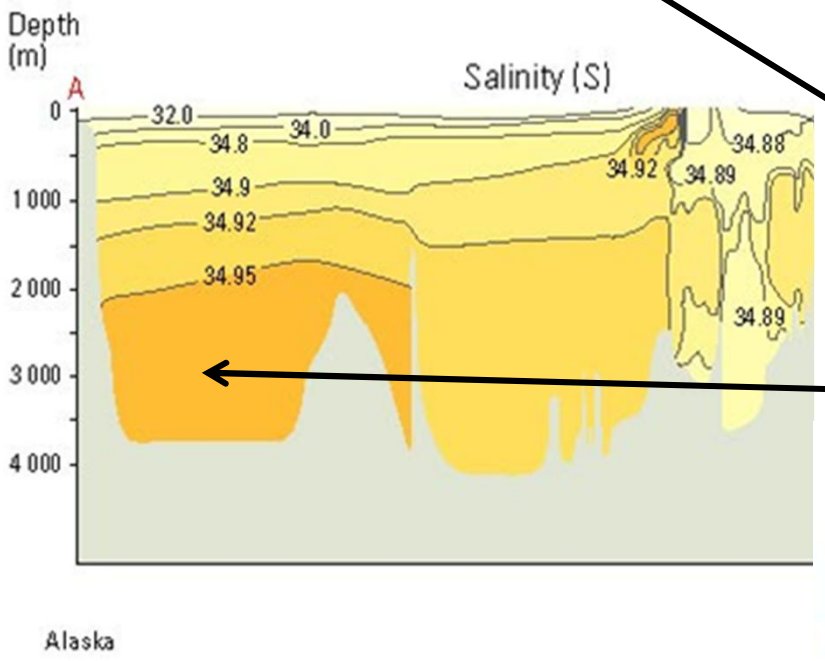
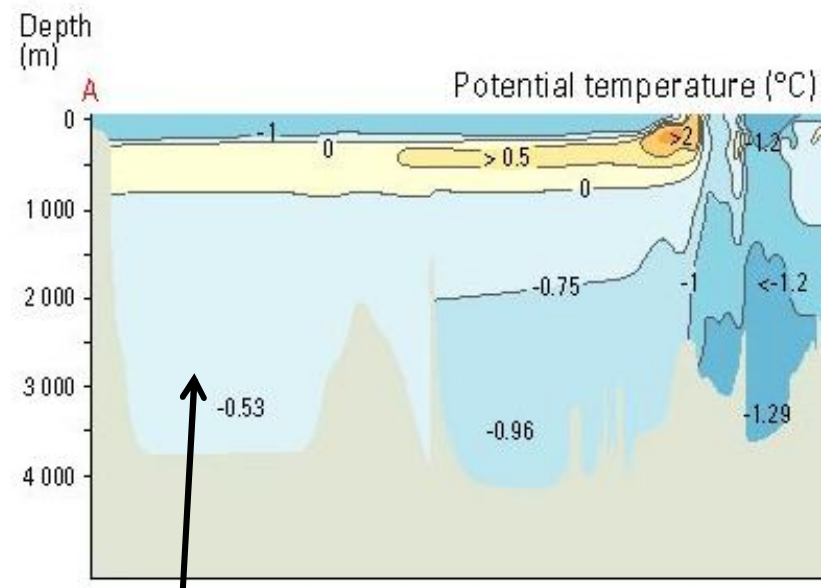
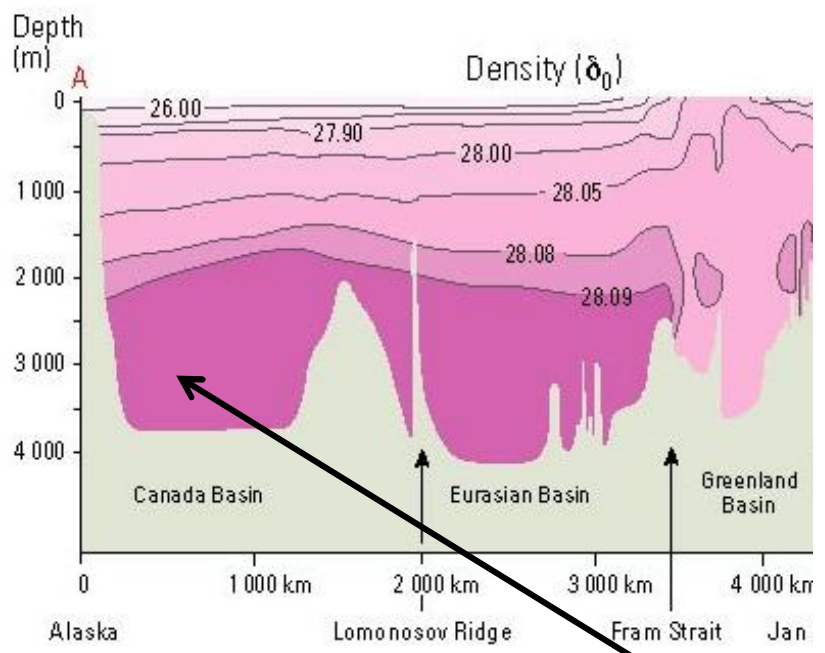
Role of dense water cascades in Arctic Ocean



Cold Halocline is maintained by influx of cold brine-enriched water from shelf. Provides a buffer layer between surface and warm Atlantic water.



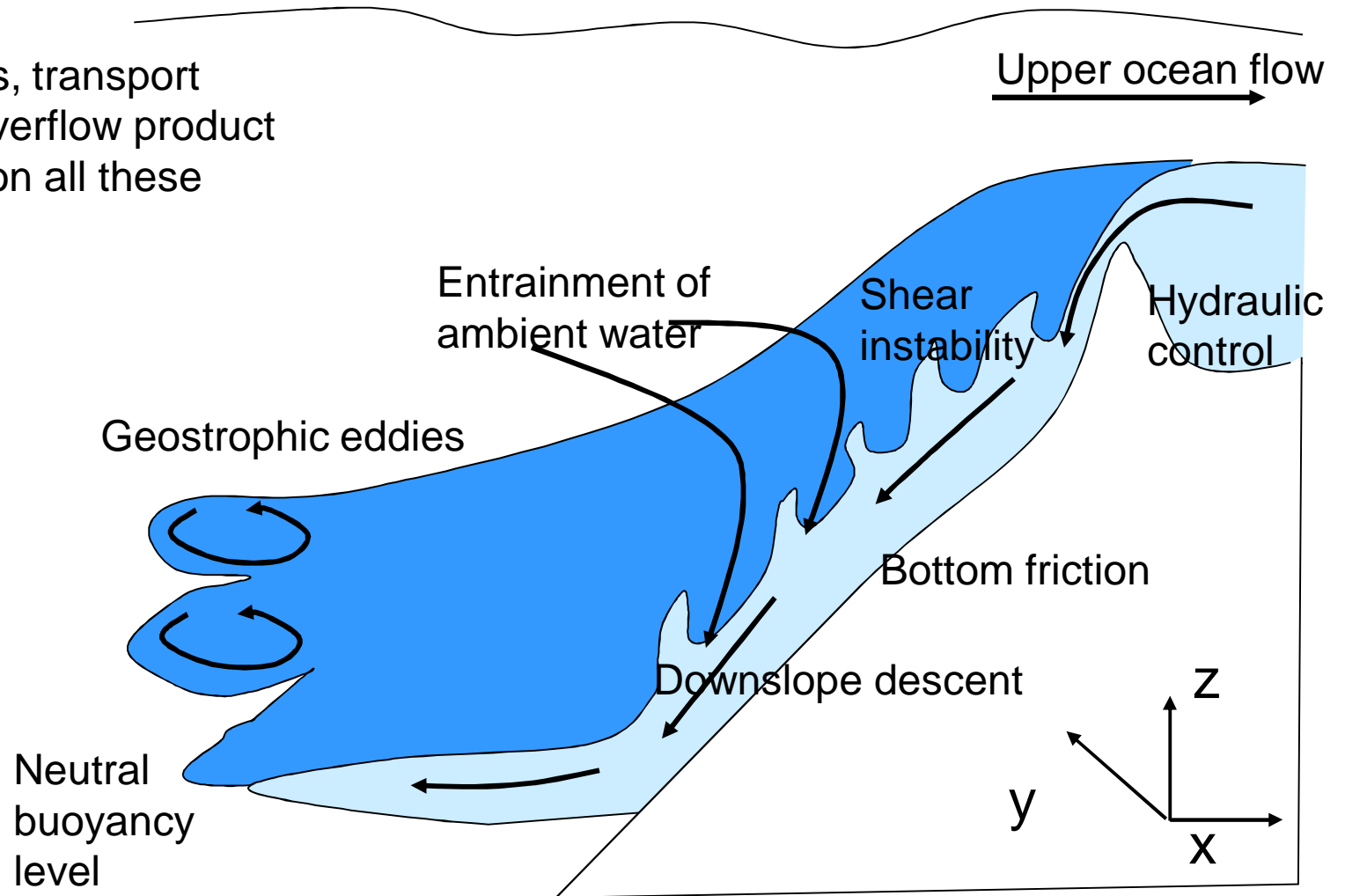
Arctic Monitoring and Assessment Programme
AMAP Assessment Report: Arctic Pollution Issues, Figure 3-30



Intermittent cascades of densest brine-enriched shelf waters supply cold saline Arctic bottom water.

Processes in overflows

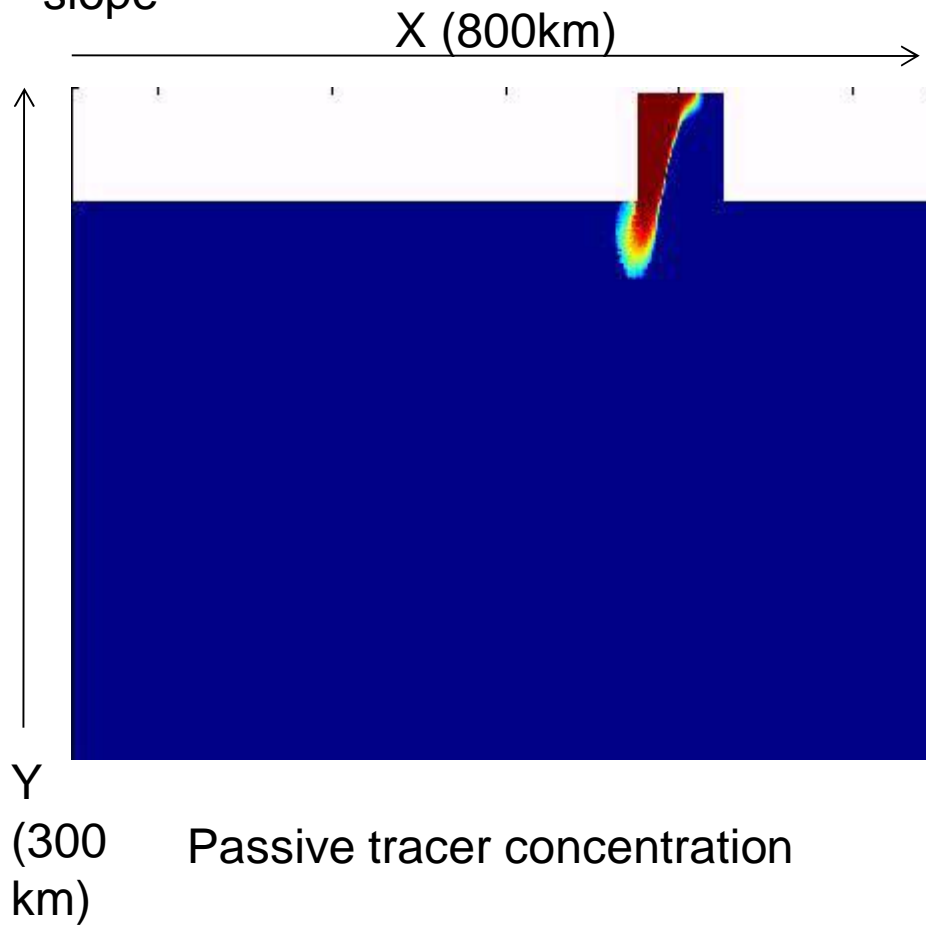
Final properties, transport and depth of overflow product water depend on all these processes.



(Legg et al, 2009)

Rotating dense overflows

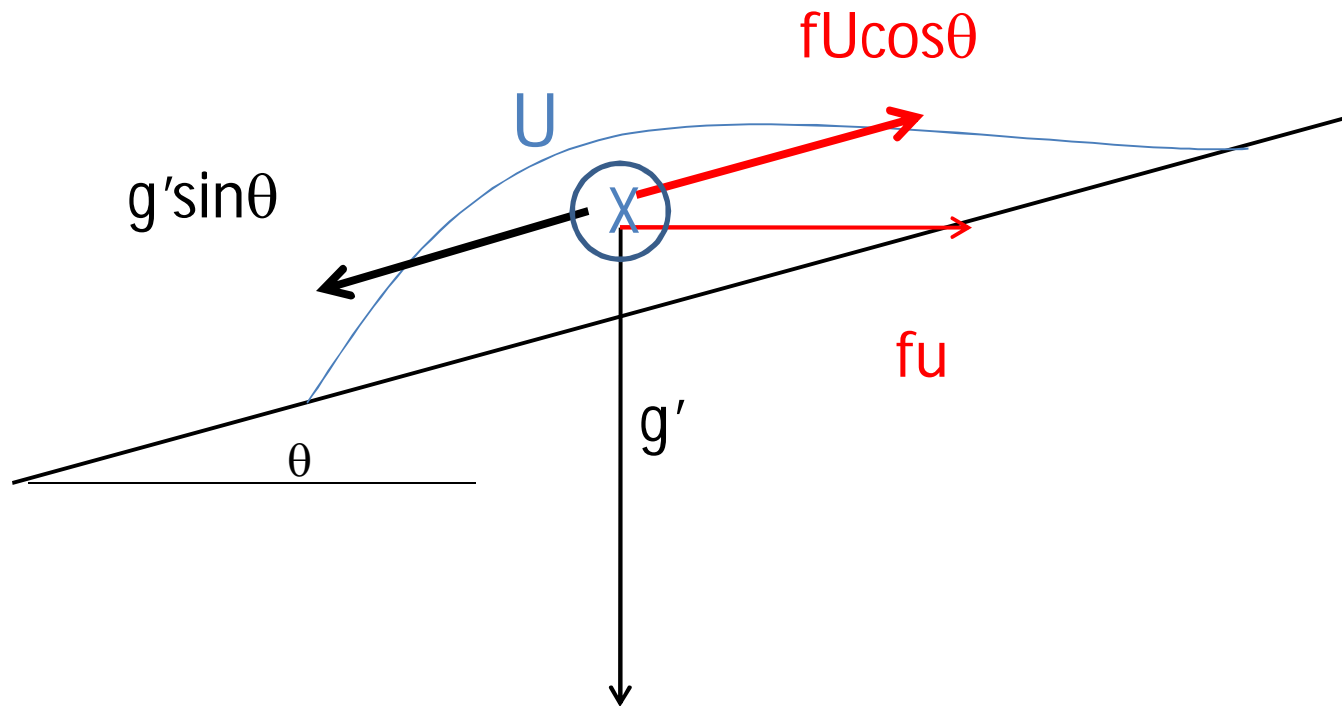
Idealized simulation of dense flow on a slope



Under influence of rotation, flow moves along isobaths. Instability leads to eddies.

(MITgcm simulation, Legg et al 2006)

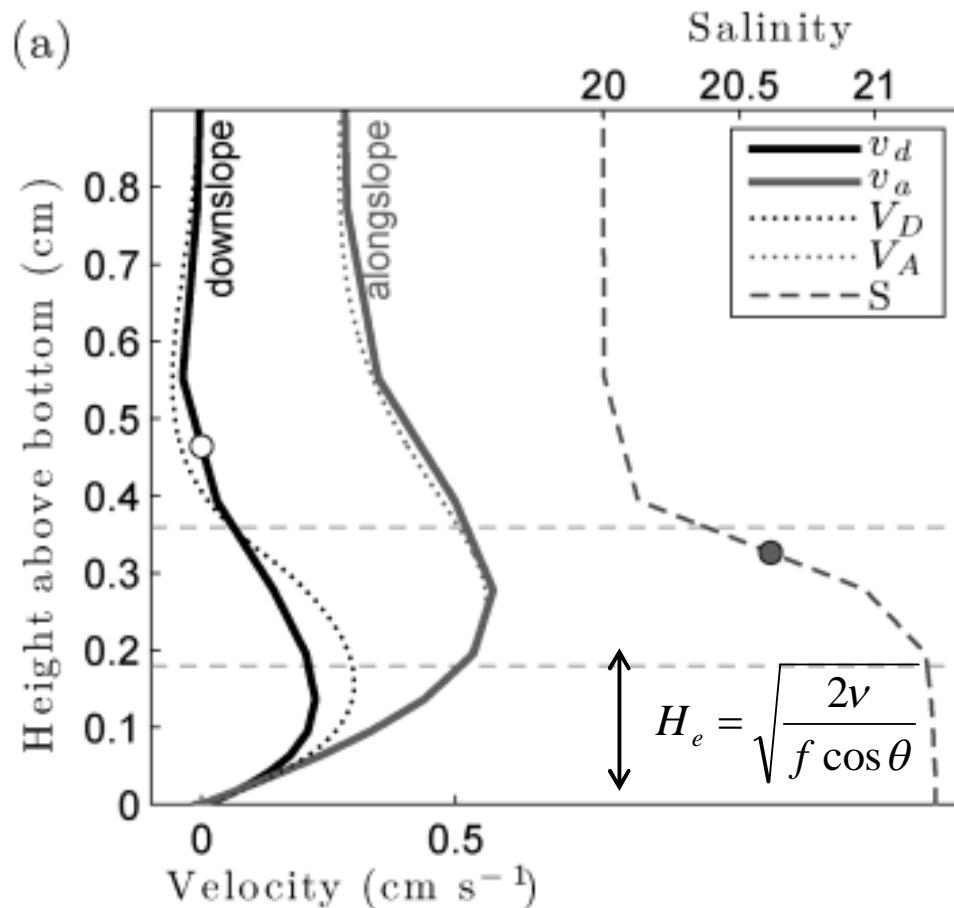
Along-isobath flow in rotating dense overflows



If flow is in geostrophic balance, then
$$U = \frac{g'}{f} \tan \theta$$

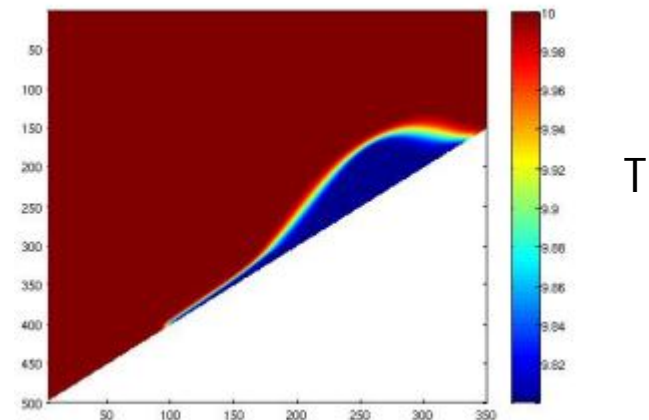
Geostrophic dense currents do not descend slope and accelerate indefinitely, but rather move along isobaths.

Effect of friction on rotating flow



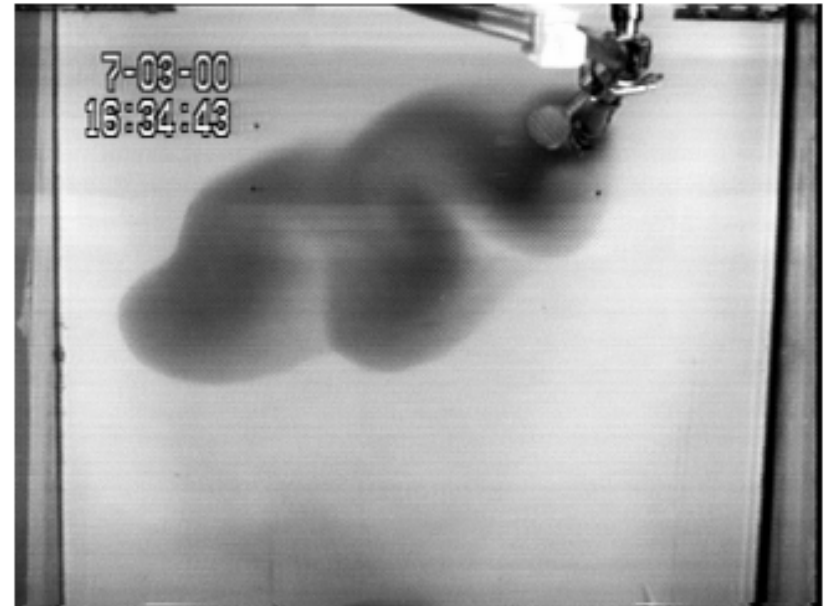
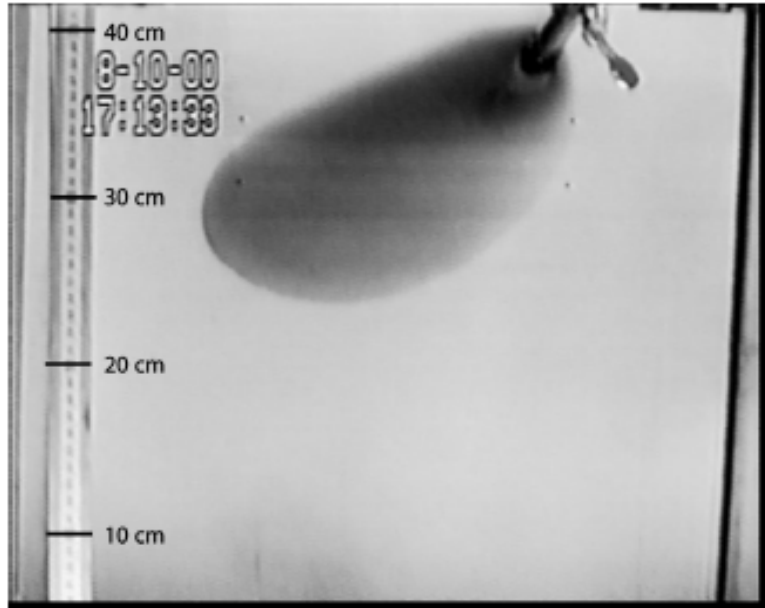
(Numerical simulations, Wobus et al, 2011)

Within bottom Ekman layer, geostrophic balance is broken, and dense fluid can move down slope.



(2D Numerical simulations, Laanaia et al 2010)

Cross-isobath transport in rotating overflows



(Cenedese et al, 2004)

Friction breaks geostrophic balance,
allowing downslope flow.

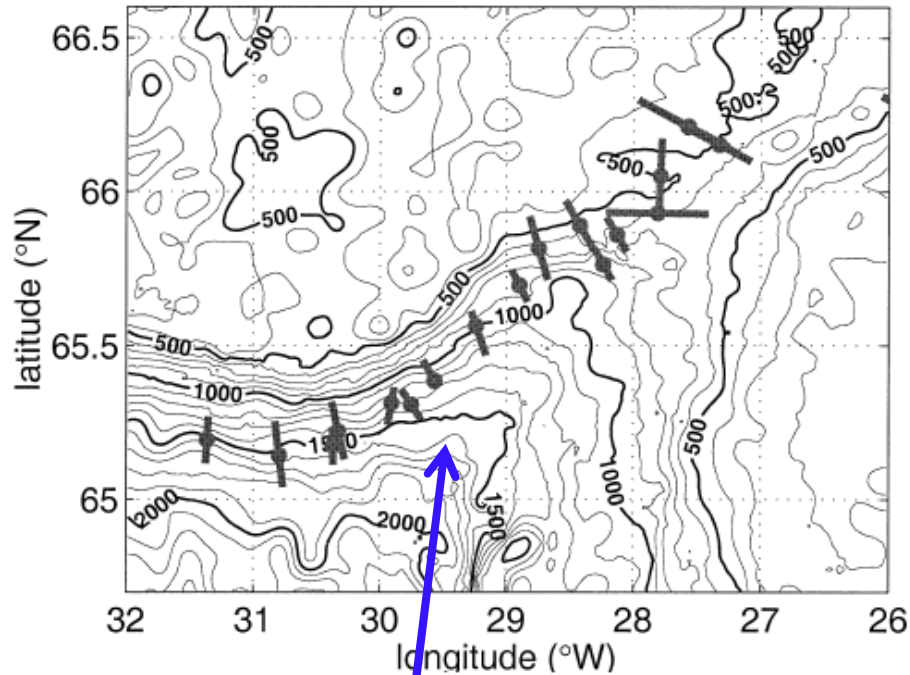
Laminar flow, no mixing, when

$$Ek = \left(\frac{\delta_E}{h} \right)^2 \geq 0.1 \quad \delta_E = \sqrt{\frac{2\nu}{f}} \quad Fr = \frac{U}{\sqrt{g'h}} < 1 \quad Ek < 0.1$$

Growing lateral instability allows
downslope (and upslope) flow .

Example: Denmark Straits overflow

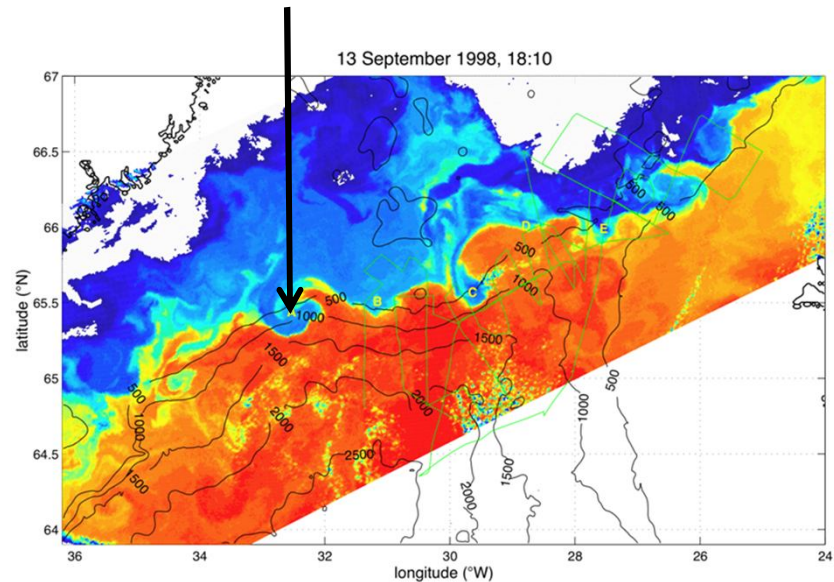
Overflow path (center of mass):
influence of friction and rotation.



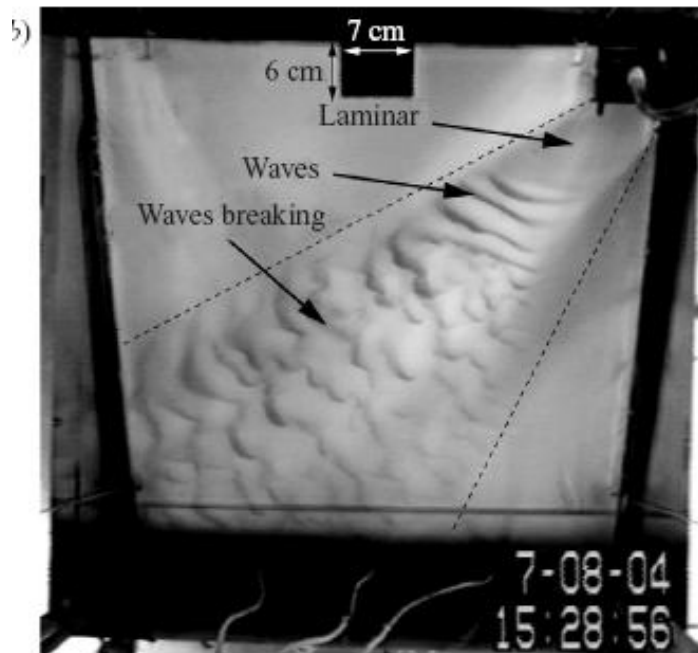
Overflow path
slowly crosses
topographic
contours

(Girton et al, 2003)

Surface cyclonic
eddies (seen in SST, *Bruce
1995*) over cold dense domes.

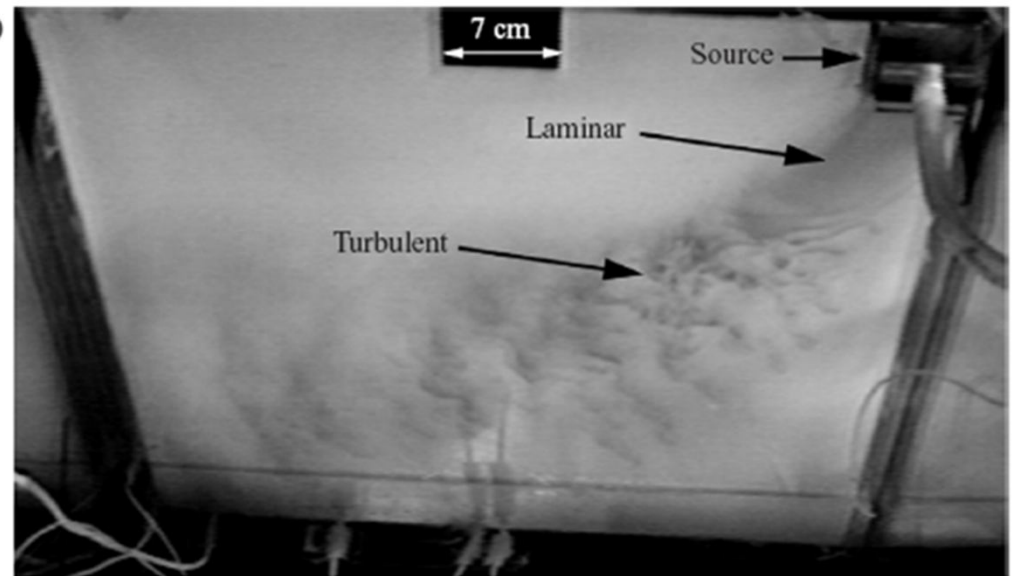


Mixing in Overflows: Roll-wave and turbulent regimes



For large Ek and moderate to large Fr , roll-wave develop, which break and cause mixing.

(Cenedese and Adduce, 2008)



For large Fr , flow is turbulent

(Cenedese et al, 2004)

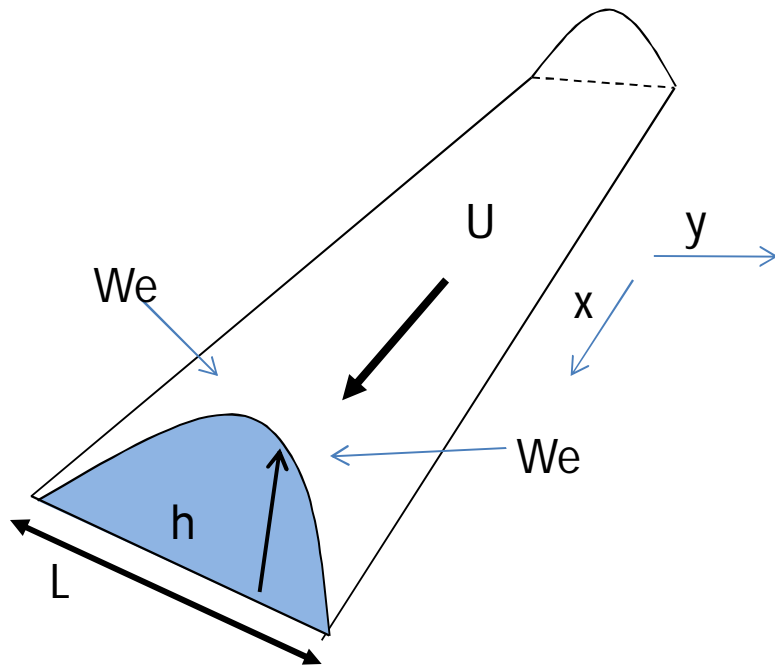
Characterizing mixing by entrainment: stream tube model of overflows

$$\frac{d}{dx} \int_L U h dy = \int_L w_e dy$$

Conservation of mass
Transport increases
due to entrainment

$$\frac{d}{dx} \int_L U h q dy = \int_L w_e q_e dy$$

Tracer conservation
Tracer properties are
diluted by entrainment



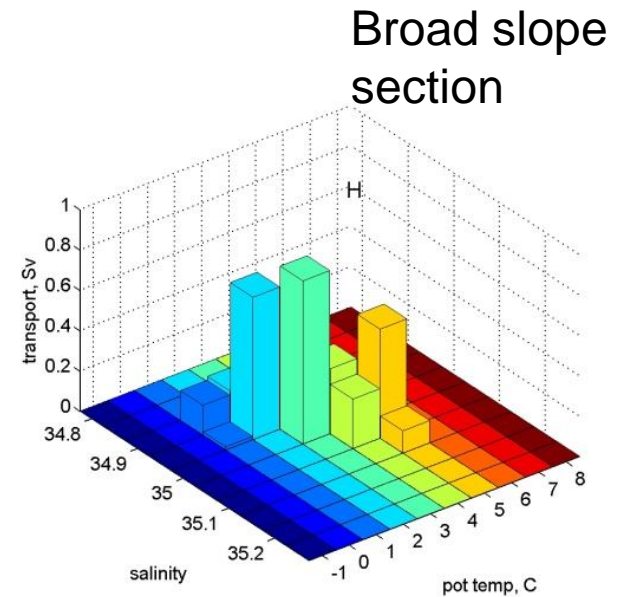
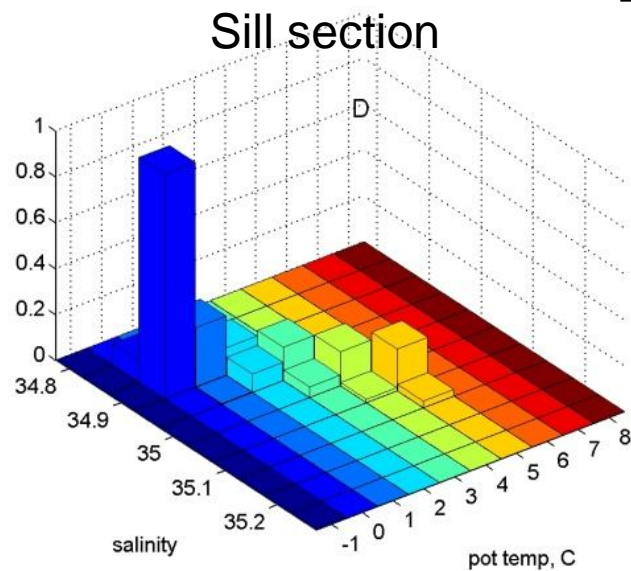
$$w_e = EU$$

Entrainment velocity

(Smith, 1975; Price and Baringer, 1994)

Entrainment in Faroe Bank Channel overflow

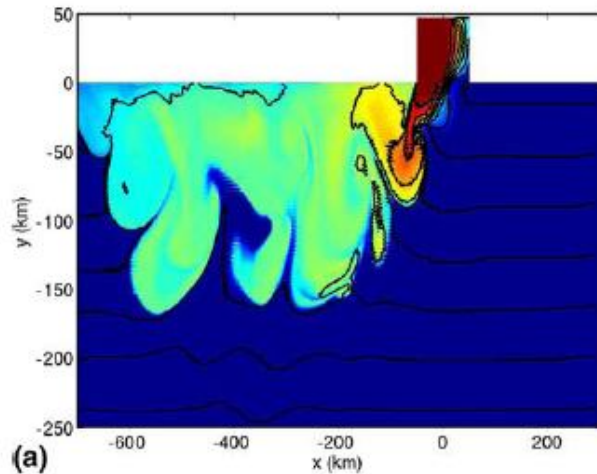
Transport in different
T,S classes



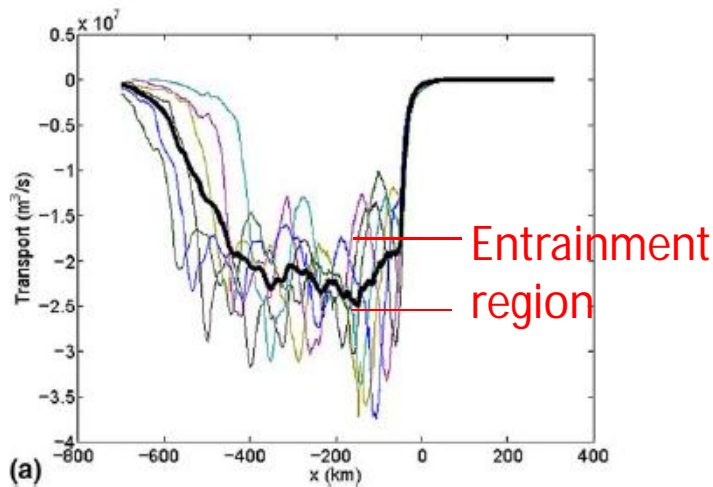
Plume becomes warmer and saltier
downstream, due to dilution.
Total transport increases.
Both are evidence of entrainment.

(Mauritzen et al 2005)

Simulation of idealized Denmark Straits-like overflow



Passive tracer at slope



Alongslope transport

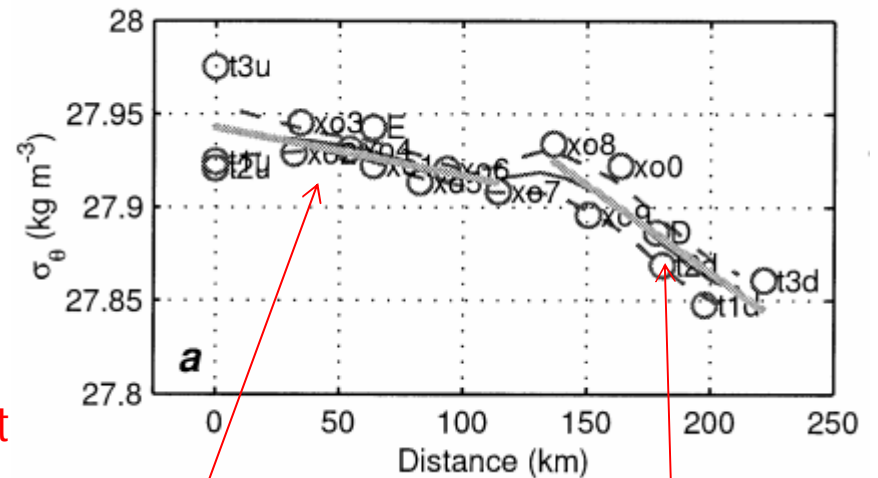
In this scenario, most entrainment occurs soon after flow exits channel.

(Legg et al, 2006)

Transport method:
$$E = \frac{w_e}{U} = \frac{\frac{d}{dx} \int_L h U dy}{UL} \approx 2 \times 10^{-3}$$

Estimating entrainment rate from numerical simulations and observations

Denmark straits observations

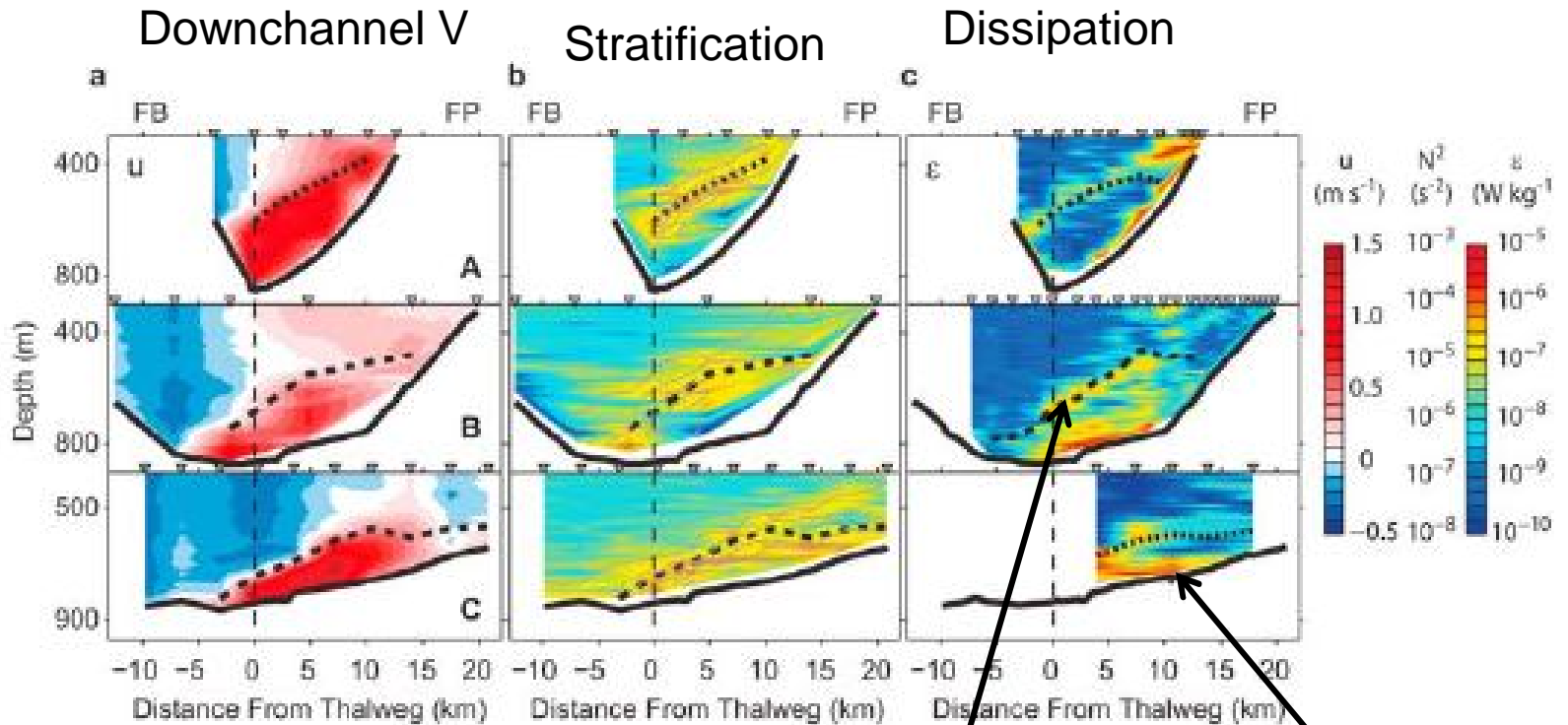


$w_e = 6 \times 10^{-5} \text{ m/s}$ $w_e = 8 \times 10^{-4} \text{ m/s}$

Tracer method:
$$w_e = \frac{Uh}{\rho'} \frac{d\sigma}{dx}$$

(Girton and Sanford, 2003)

Where do dissipation and mixing occur in Faroe Band Channel overflow?



Dissipation in stratified interfacial shear layer

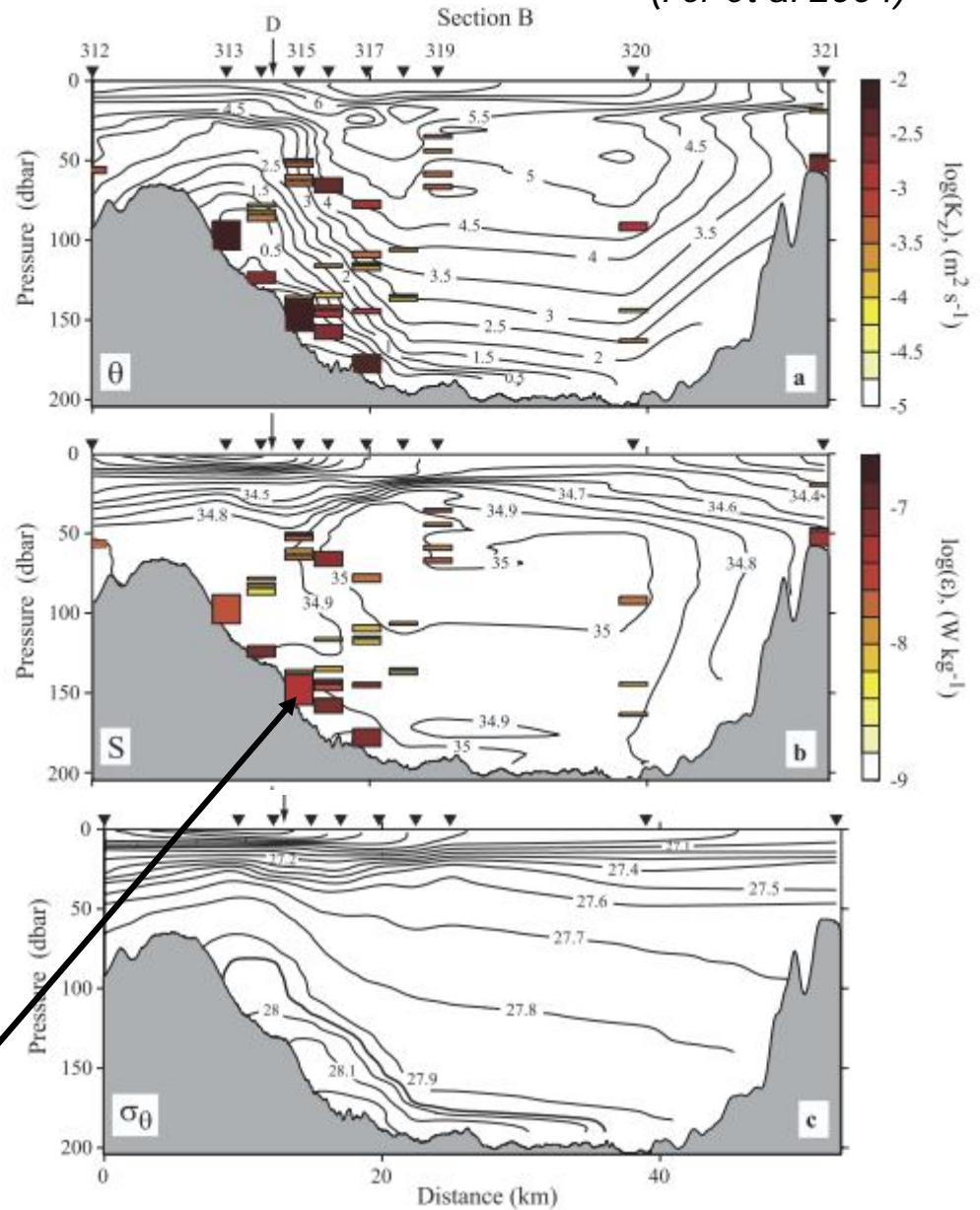
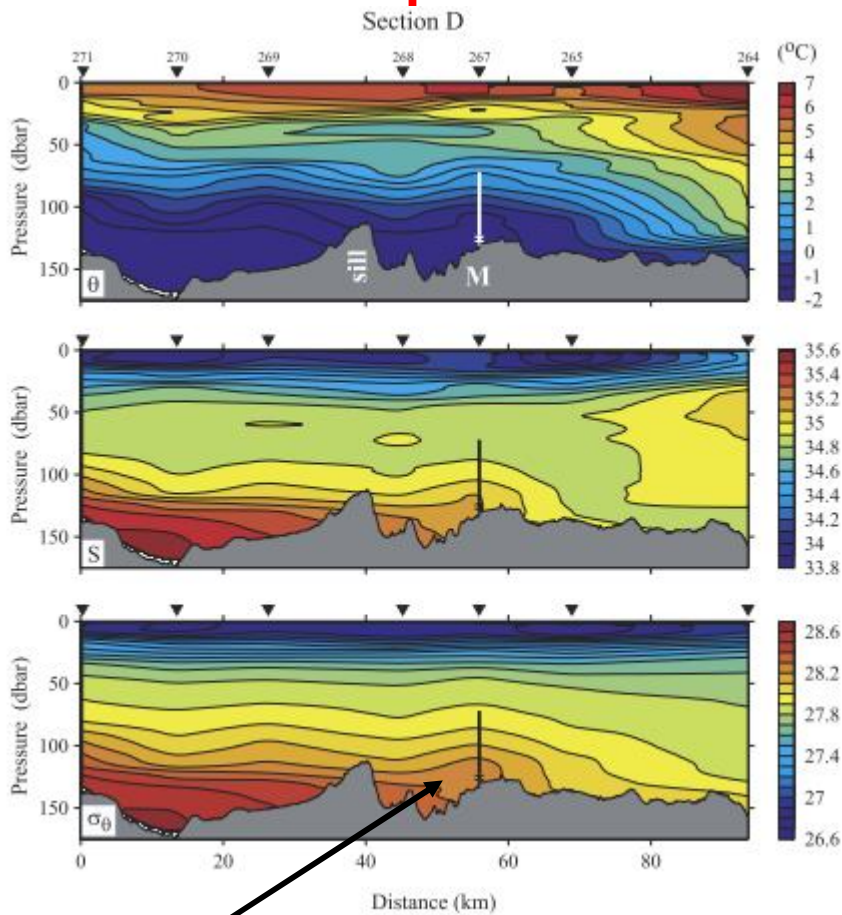
Dissipation in frictional boundary layer

(Fer et al, 2004)

Two different locations of dissipation/mixing

Turbulence and mixing in Storfjorden overflow plume

(Fer et al 2004)



Downstream development: temperature, salinity and density become diluted.
Cross-section shows elevated dissipation in dense plume layer.

Entrainment mechanisms

2D nonrotating simulation:
(Ozgokmen and Chassignet, 2002)

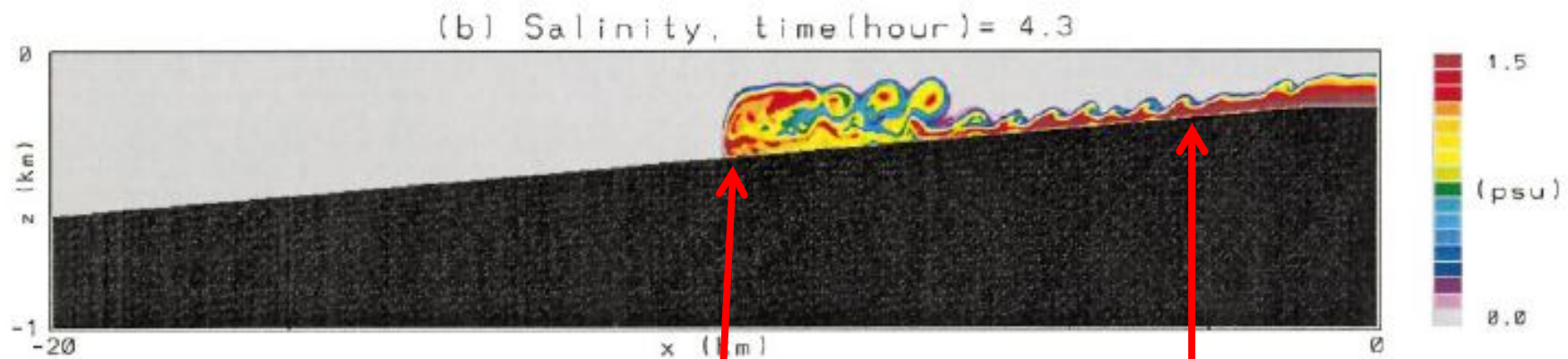


FIG. 2. Snapshots of the salinity distribution in (a) expt 3 ($\Delta S = 3.0$ psu and $\theta = 5^\circ$) and (b) expt 4 ($\Delta S = 1.5$ psu and $\theta = 1^\circ$).

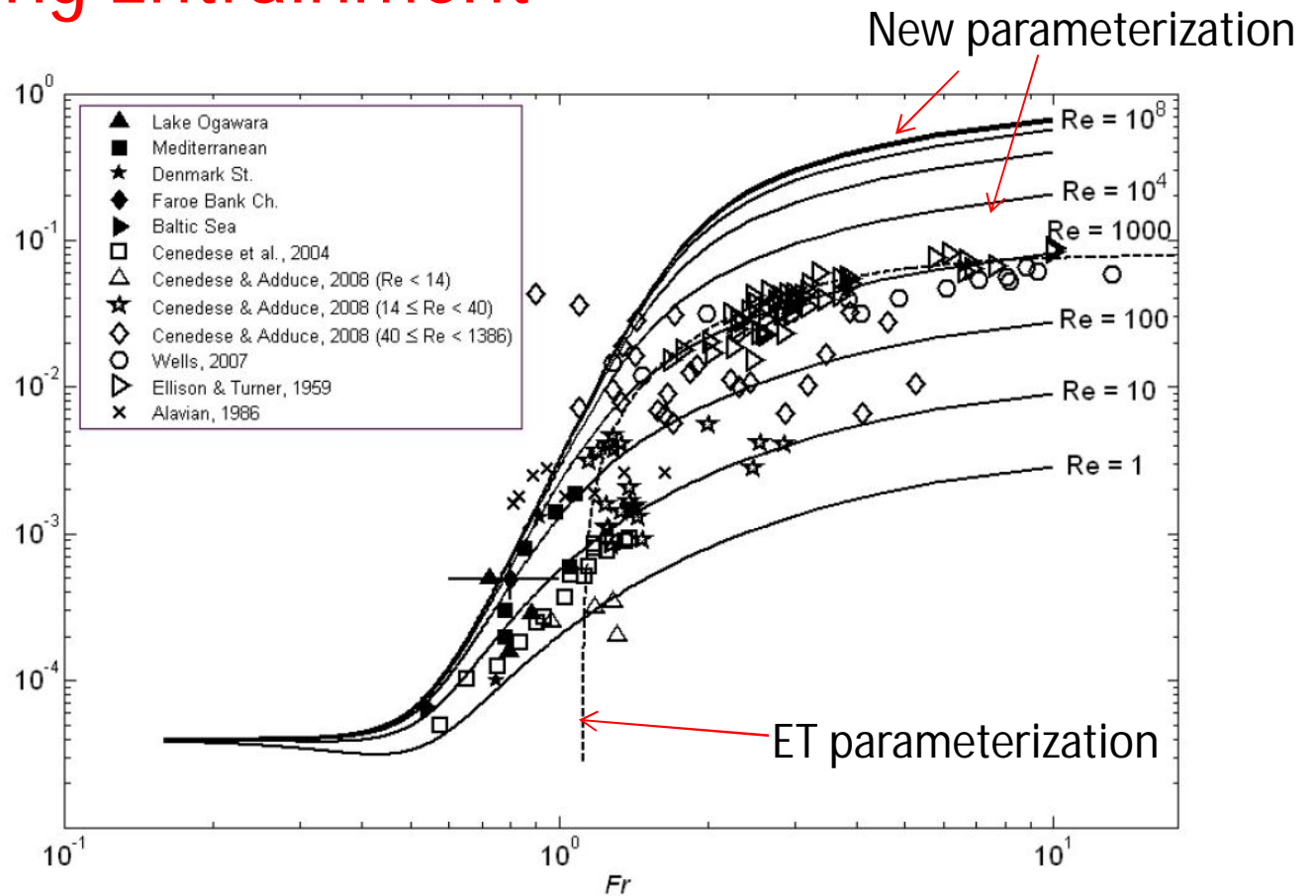
Gravity current head

Kelvin-Helmholtz
billows in tail

For oceanic overflows in quasi-steady state, the Kelvin-Helmholtz billows in the extended tail are more relevant.

Parameterizing Entrainment

In a bulk view of the overflow plume, entrainment is parameterized in terms of bulk properties such as Froude number and Reynolds number



$$E = \frac{0.08Fr^2 - 0.1}{Fr^2 + 5} \quad \text{for} \quad Fr^2 \geq 1.25 \quad (\text{Ellison and Turner, 1959})$$

New parameterization

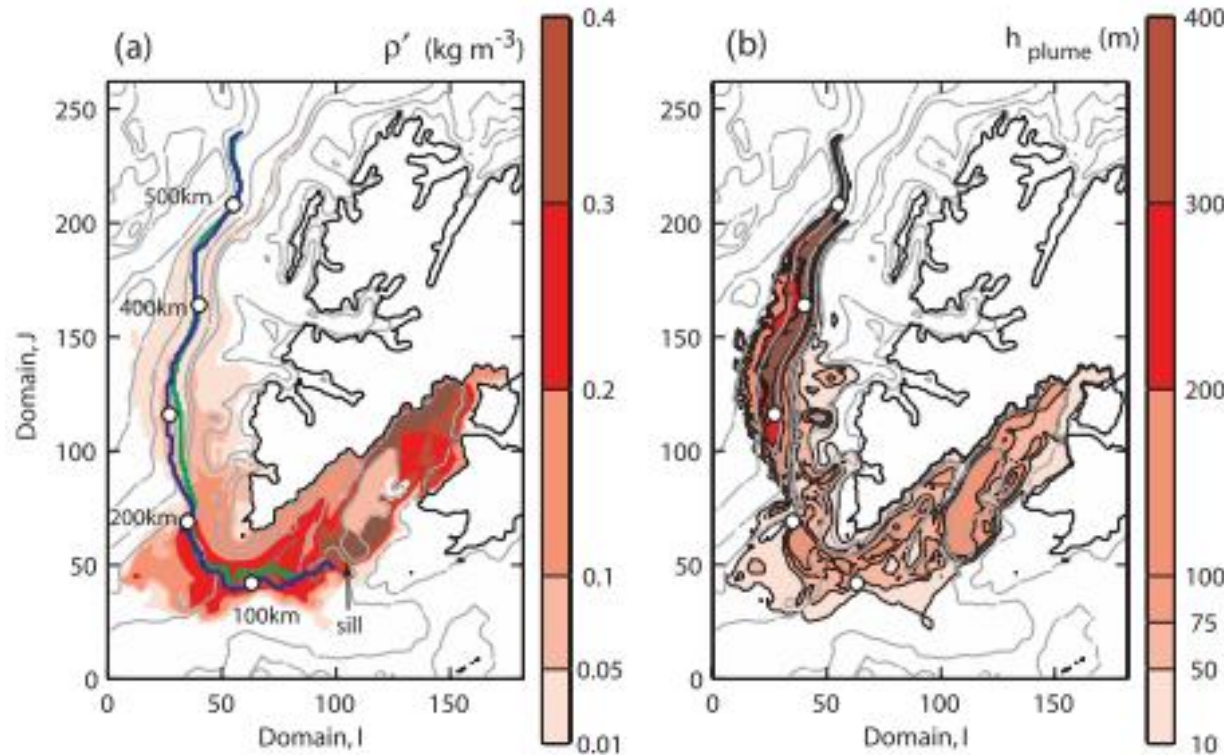
$$E = \frac{E_{\min} + A Fr^\alpha}{1 + AC_{\text{inf}} (Fr + Fr_0)^\alpha} \quad C_{\text{inf}} = \frac{1}{E_{\max}} + \left(\frac{B}{Re^\beta} \right)$$

(Cenedese and Adduce, 2010)

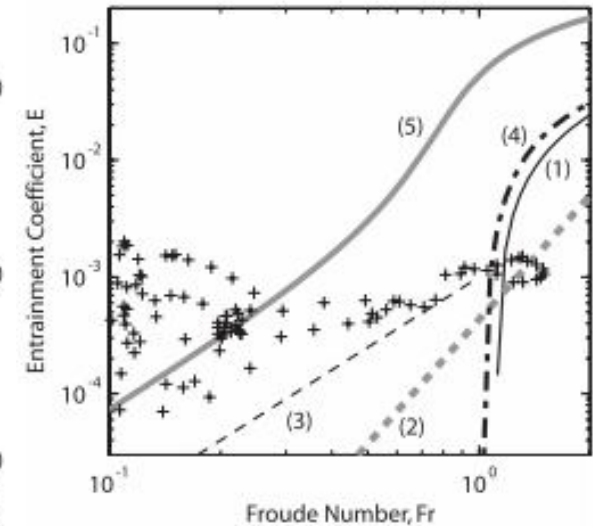
Entrainment in Storfjorden

Simulations using ROMS with M-Y 2.5 mixing parameterization.

(Fer and Adlandsvik, 2008)



Bottom density and plume thickness



Diagnosed entrainment:
little Fr dependence found.

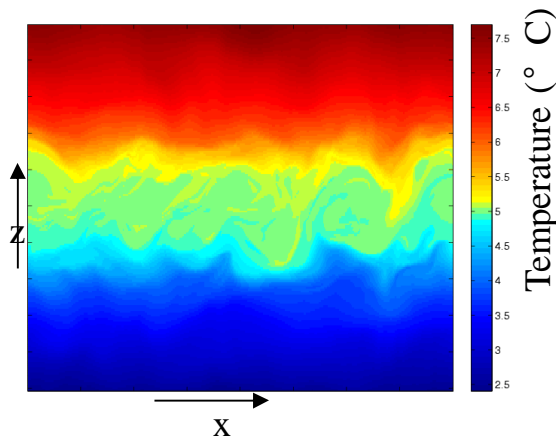
Models with Richardson number dependent mixing parameterizations (e.g. M-Y 2.5, k-epsilon) seem to give reasonable agreement with observations; produce mixing even when bulk $Fr < 1$. Comprehensive parameterization of mixing in overflows still needs further development/verification.

Example of new parameterization of shear-driven mixing

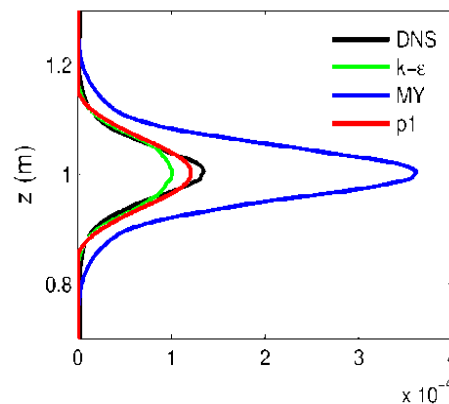
$$\frac{\partial^2 \kappa}{\partial z^2} - \frac{\kappa}{L_B^2} = -2 SF (Ri)$$

$$F(Ri) = \frac{0.15(1 - Ri / Ri_c)}{(1 - 0.9 Ri / Ri_c)}$$

where S is the vertical shear of the resolved horizontal velocity, and $L_B = Q^{1/2} / N$ is the buoyancy length scale (the scale of the overturns), N is the buoyancy frequency, and Q is the turbulent kinetic energy, found from an energy budget.



3D high res simulation
MITgcm



Diffusivities diagnosed from simulation and predicted by different parameterizations (new parameterization = p1)

New parameterization contains no dimensional constants. Tuned by comparison with lab expts & high res. numerical simulations.

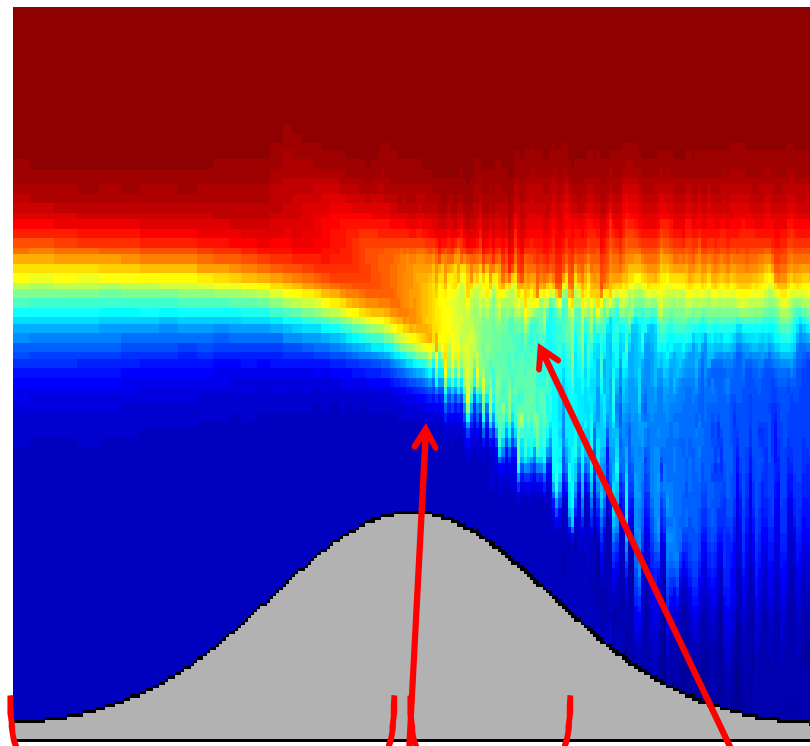
Could be modified to include low Fr (high Ri) mixing and Re dependence.

(Jackson, Hallberg, and Legg, 2008).

Fr/Ri dependence is still empirical:
fundamental understanding needed

Topographic effects: Mixing in hydraulic jumps

Temperature



Subcritical flow

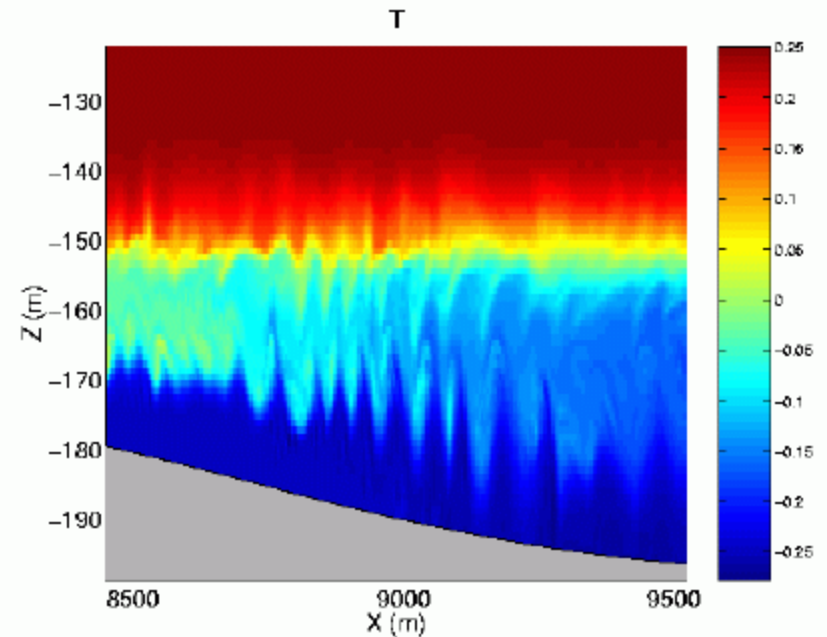
$$Fr = \frac{U}{\sqrt{g'h}} < 1$$

Supercritical flow

$$Fr = \frac{U}{\sqrt{g'h}} > 1$$

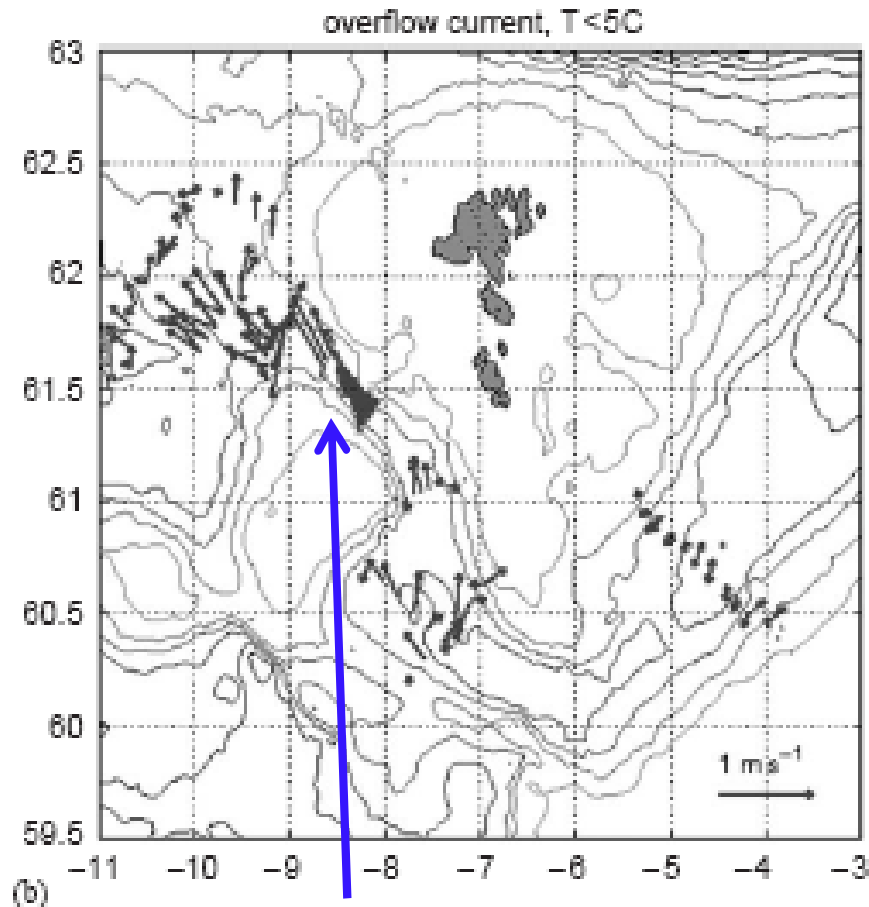
Transition at sill:
hydraulic control

Transition to subcritical
flow: hydraulic jump



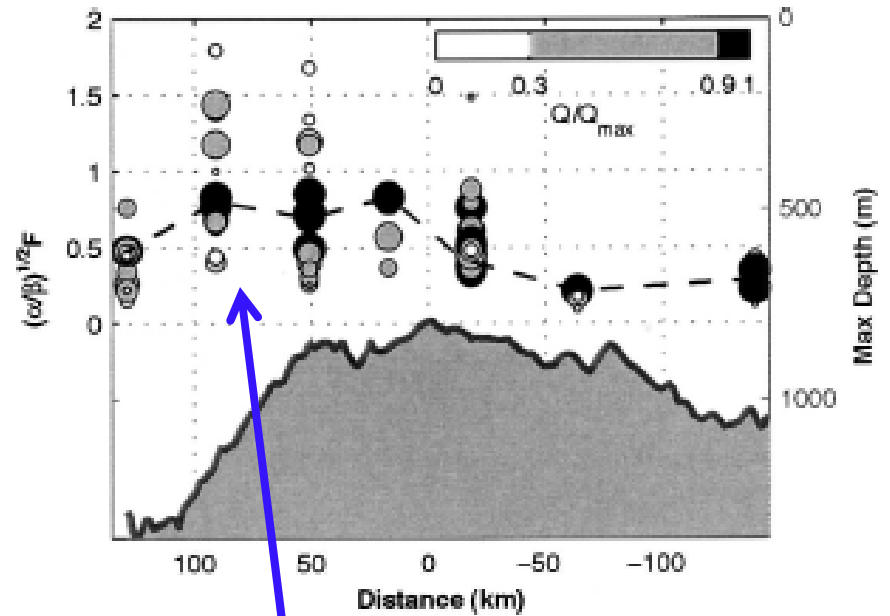
Kelvin-Helmholtz billows
in transition region

Hydraulic effects in Faroe Bank Channel overflow



Accelerated flow in channel and on slope

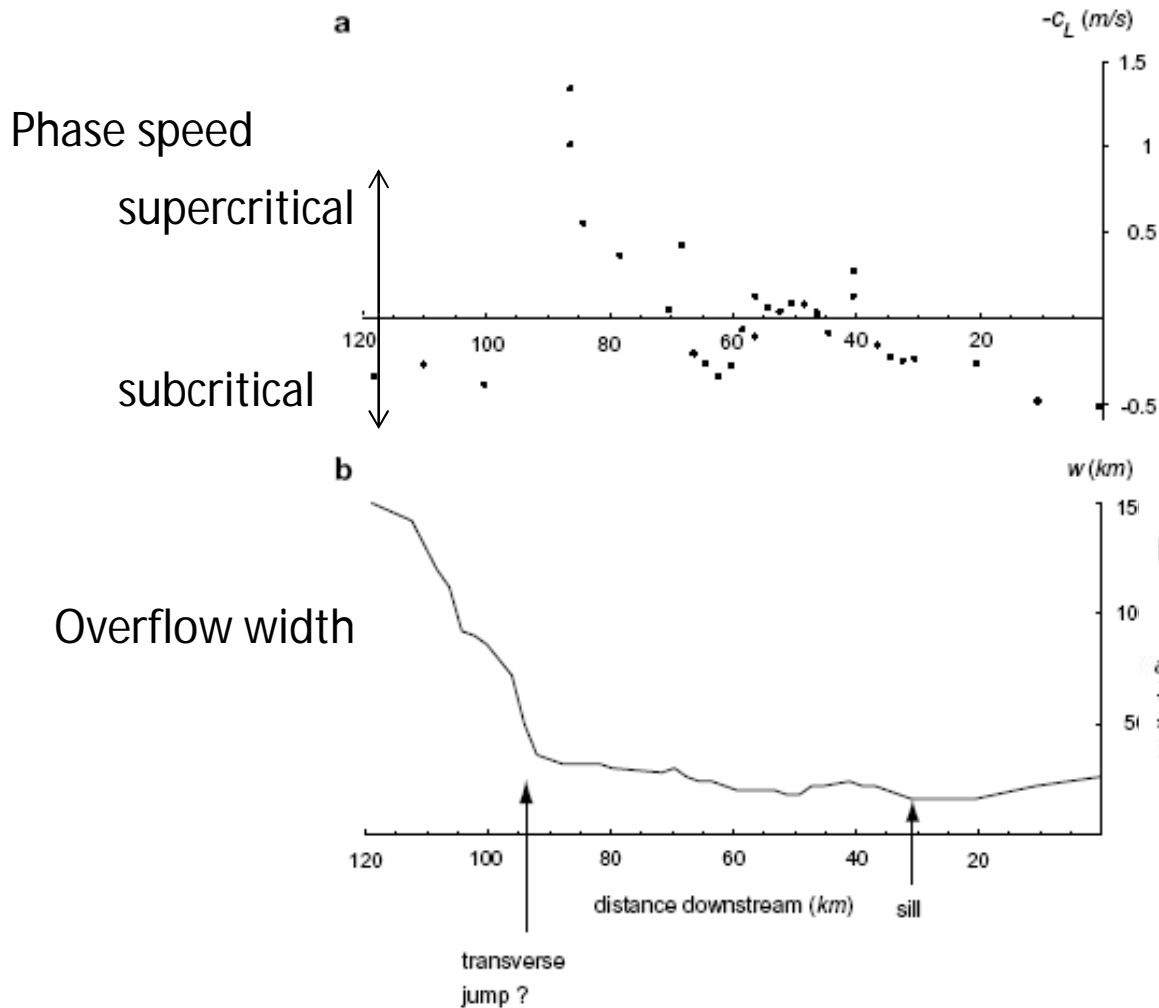
(Mauritzen et al, 2005)



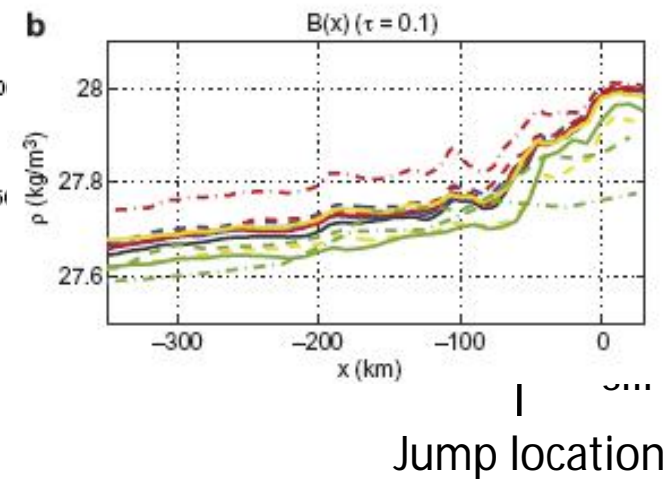
Large velocities and thin layer -> Froude numbers close to 1

(Girton et al, 2006)

Faroe Bank Channel: transverse hydraulic jumps in presence of rotation



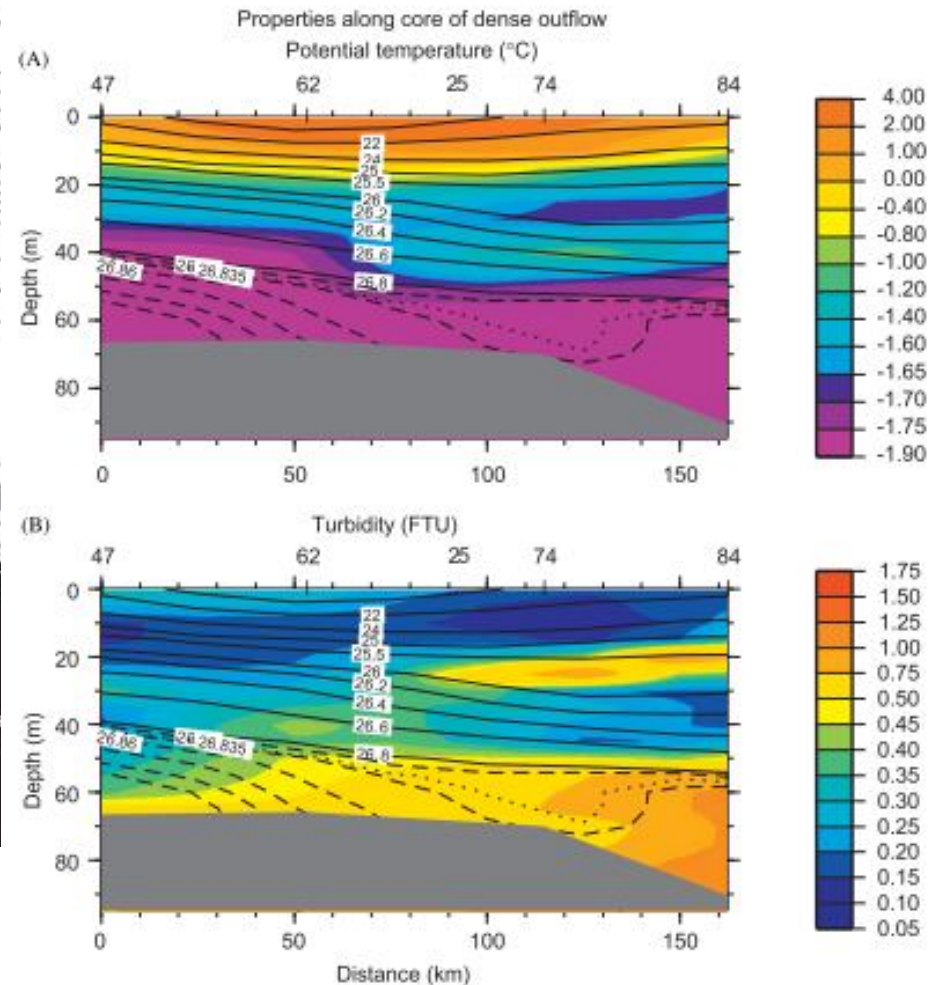
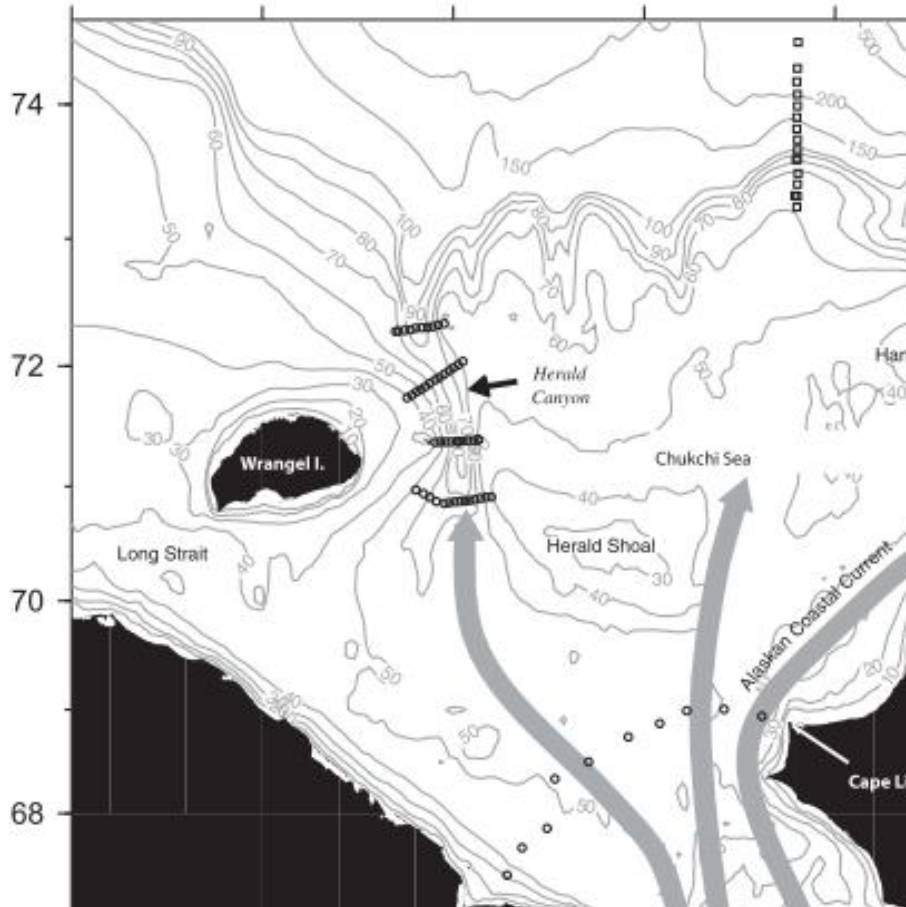
Transition from supercritical to subcritical state leads to sudden widening of current, also associated with change in mixing regime.



(Pratt et al, 2007, numerical simulations of Faroe Bank Channel overflow)

(Riemenschneider and Legg, 2007)

Hydraulic jump in Herald Canyon, Chukchi Sea



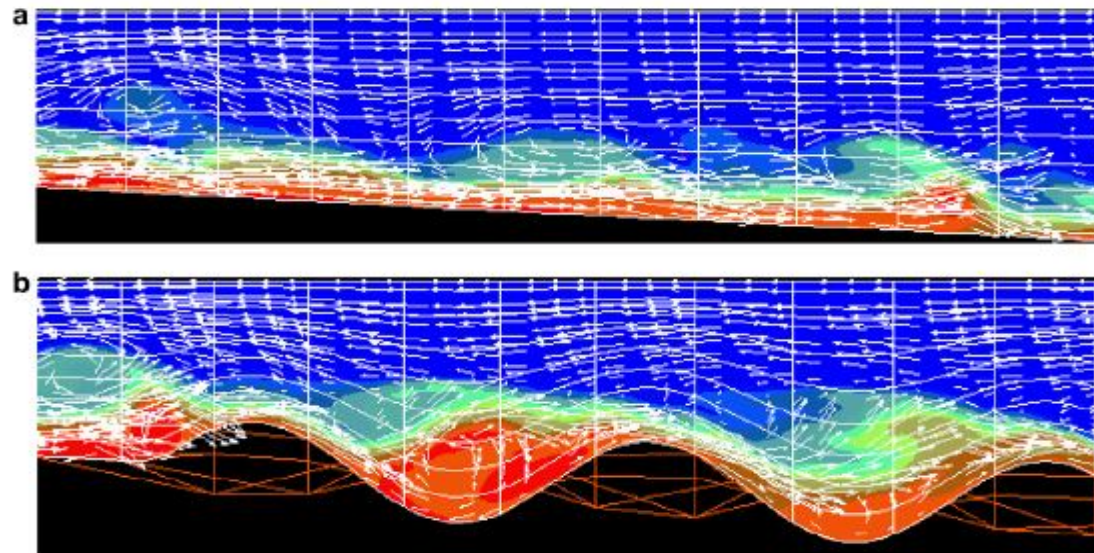
(Pickart et al, 2010)

Increase in turbidity is associated with jump-like feature in density

Other influences of topography: enhancement of entrainment

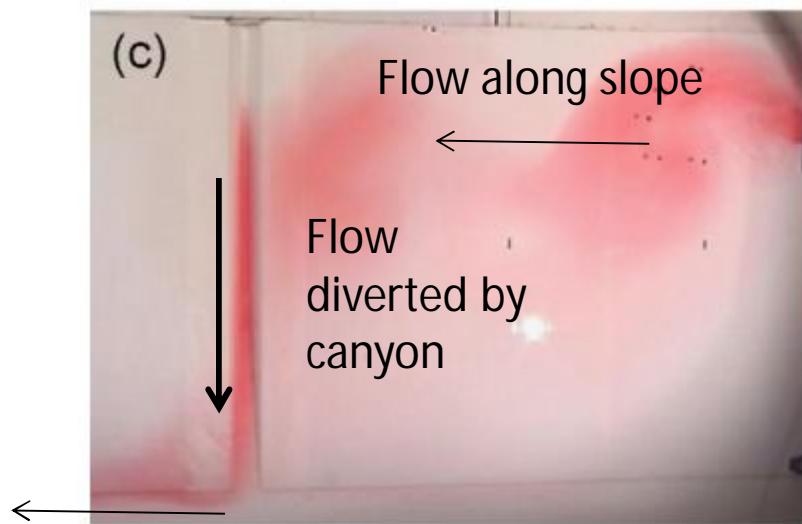
Salinity and velocity from 3D nonrotating simulations

(Ozgokmen et al, 2008)



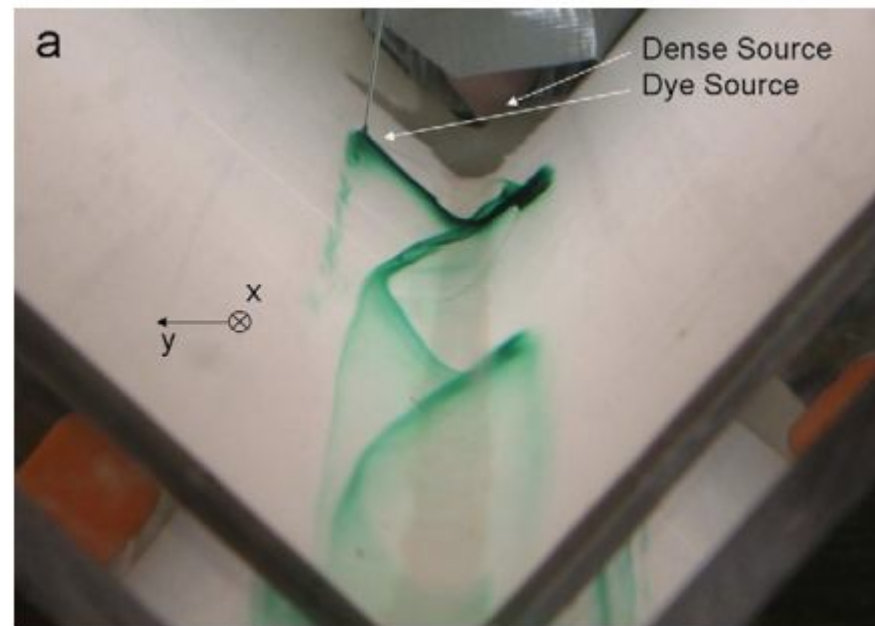
When roughness height \rightarrow dense layer thickness, then entrainment is enhanced.

Canyons: enhanced downslope transport



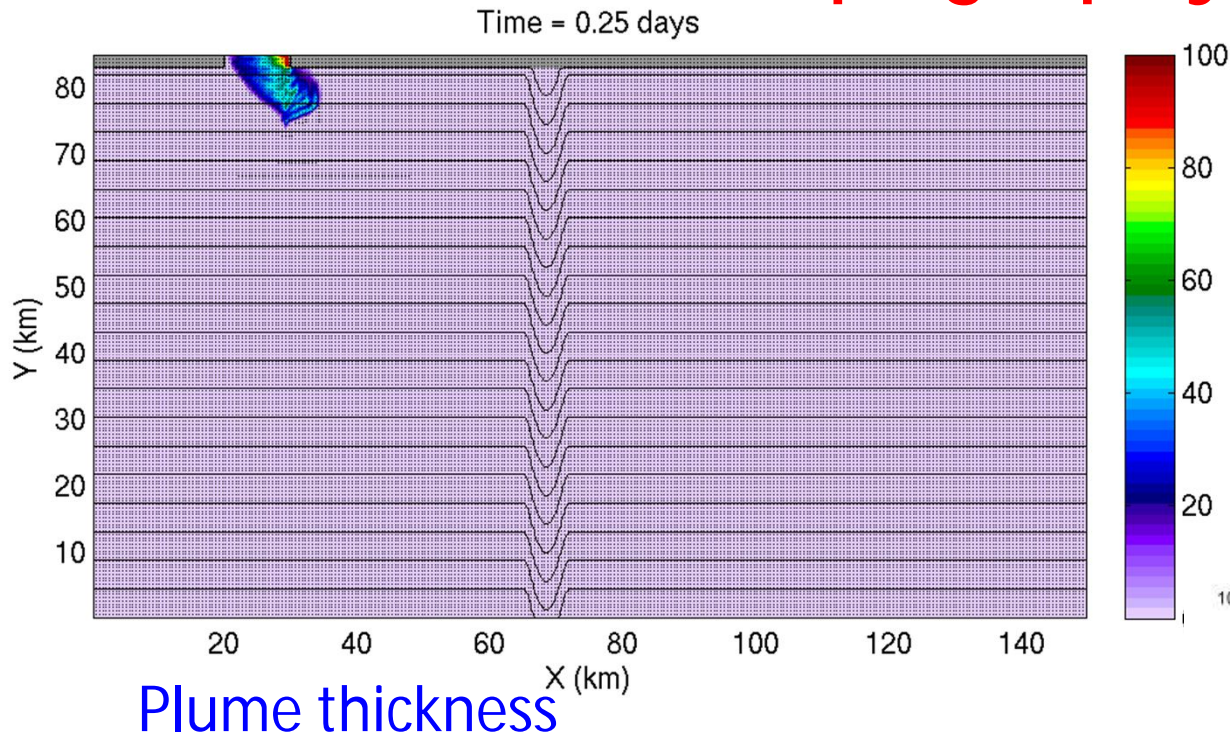
(Wahlin et al 2008)

Ekman spiral secondary circulation within V-shaped canyon



(Darelius 2008)

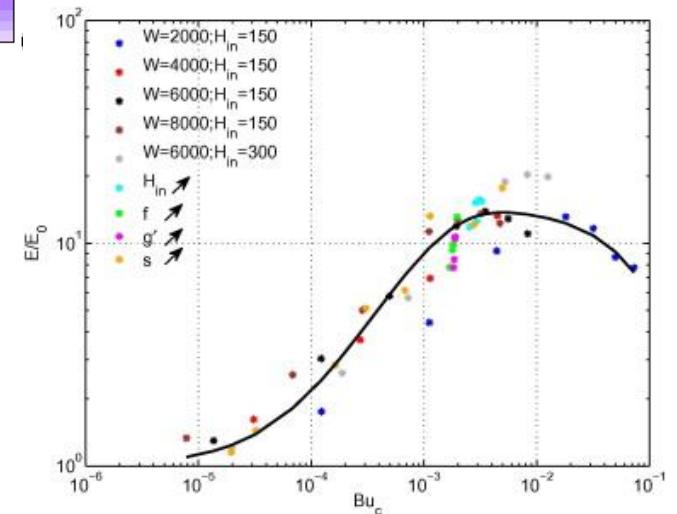
Enhancement of entrainment by small-scale topography



(Ilicak et al, 2011)

Entrainment v.

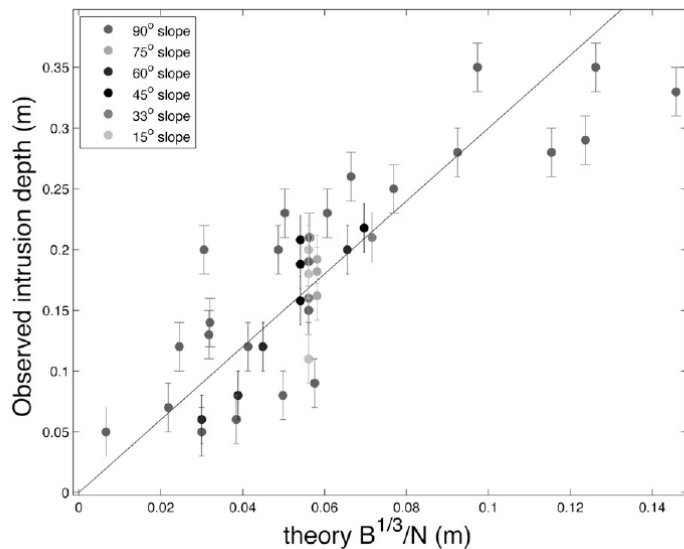
$$Bu_c = \frac{H^2}{W^2} \frac{1}{s^2} \frac{H_0}{g' / f^2}$$



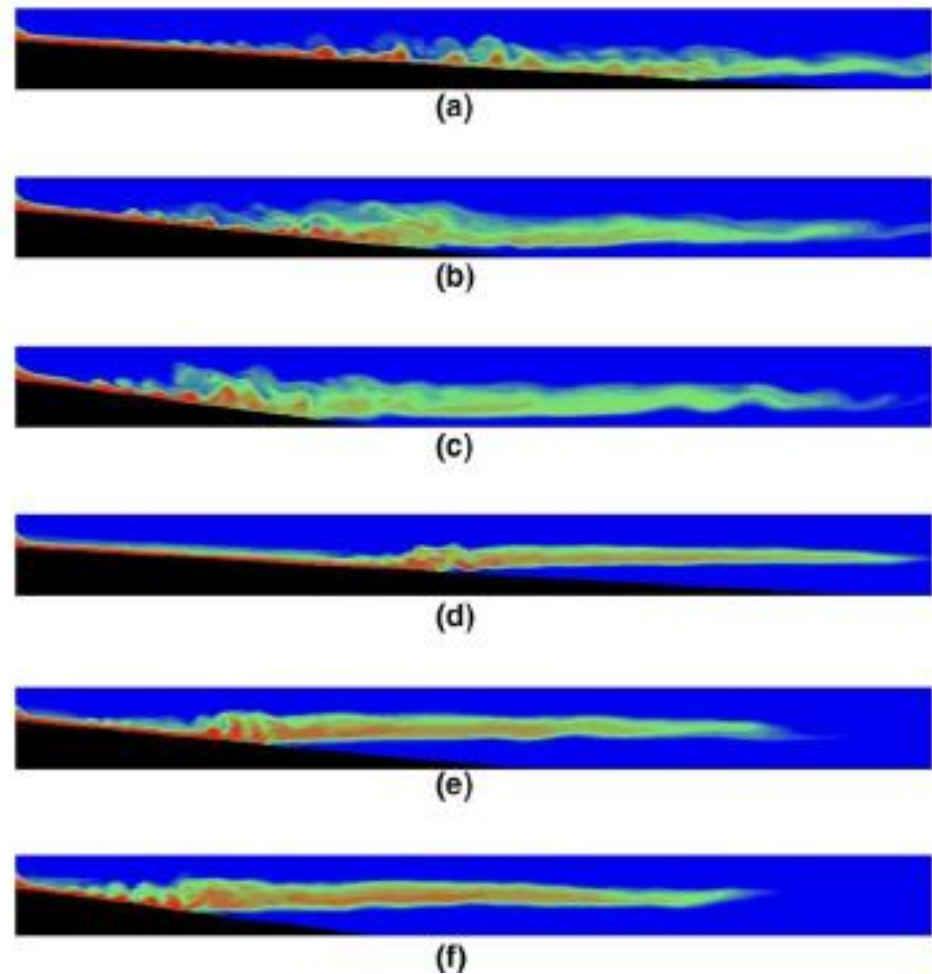
Detrainment: when overflow plume reaches neutral buoyancy level

Salinity for different slope angles and stratification

Intrusion depth depends on ambient stratification, initial buoyancy of plume, entrainment.

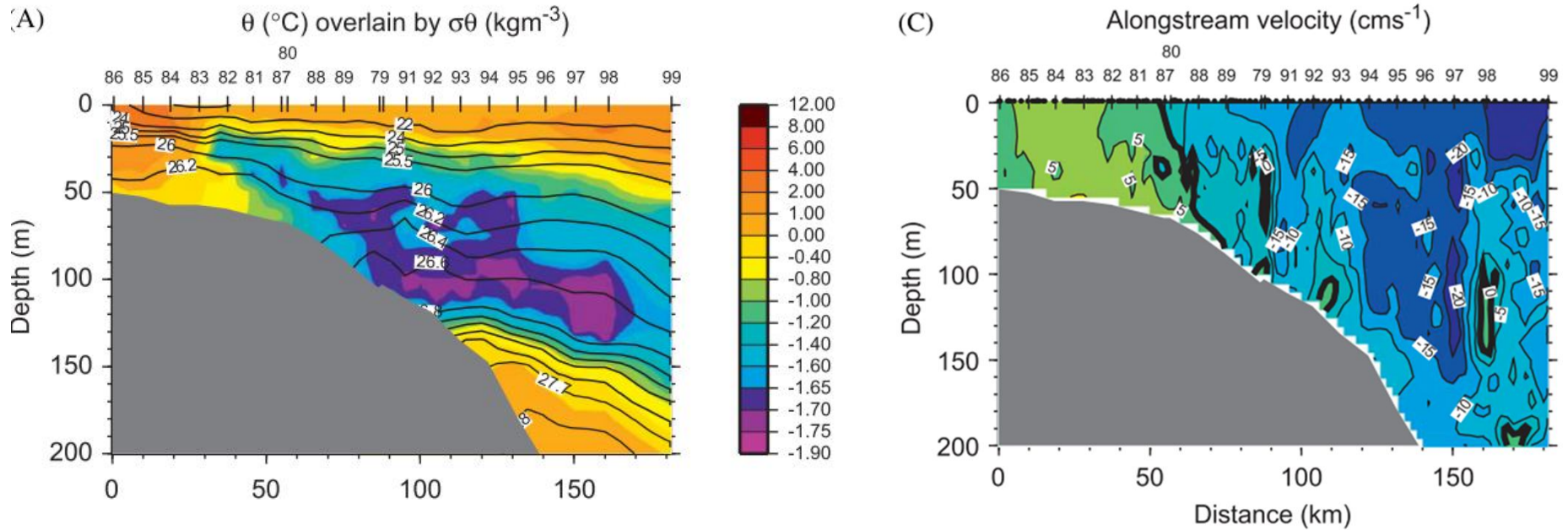


(Lab expts, Wells and Nadarajah, 2009)



(Simulations, Ozgokmen et al, 2006)

Chukchi Slope detrainment



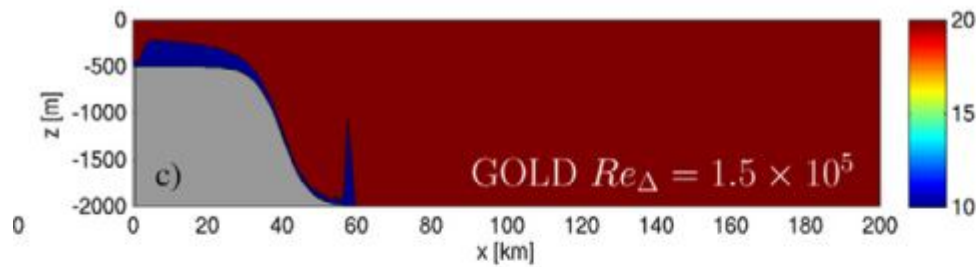
Under influence of rotation, detrainment generates subsurface eddies.

(Pickart et al, 2010)

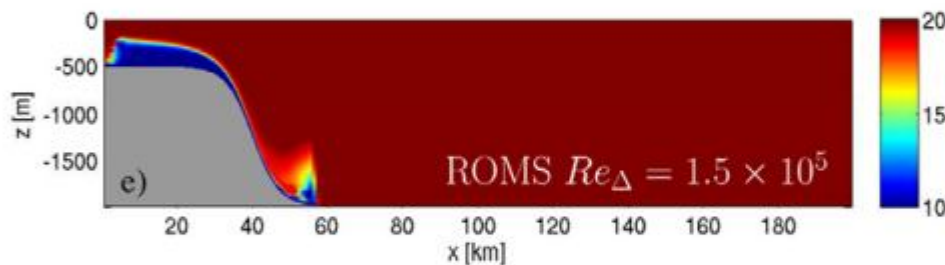
Summary of overflow processes

- **Downslope descent:** Geostrophic dense plume tends to flow along isobaths, with cross-slope transport induced by friction and instability eddies.
- **Entrainment:** Turbulence induced by shear in frictional boundary layer and interfacial layer, leads to entrainment of ambient water, dilution of plume.
- **Topographic effects:** hydraulic control, small-scale topography influence entrainment and descent.
- **Detrainment:** Plume separates from topography on reaching neutral buoyancy level, dependent on initial buoyancy deficit, total entrainment and ambient stratification.

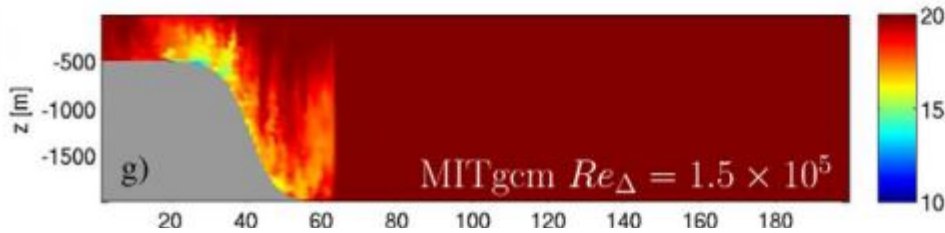
Some Modeling Considerations



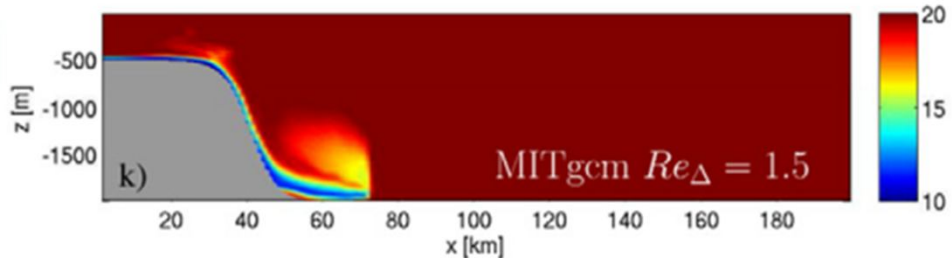
Isopycnal coordinates



σ -coordinates, dissipative momentum advection scheme



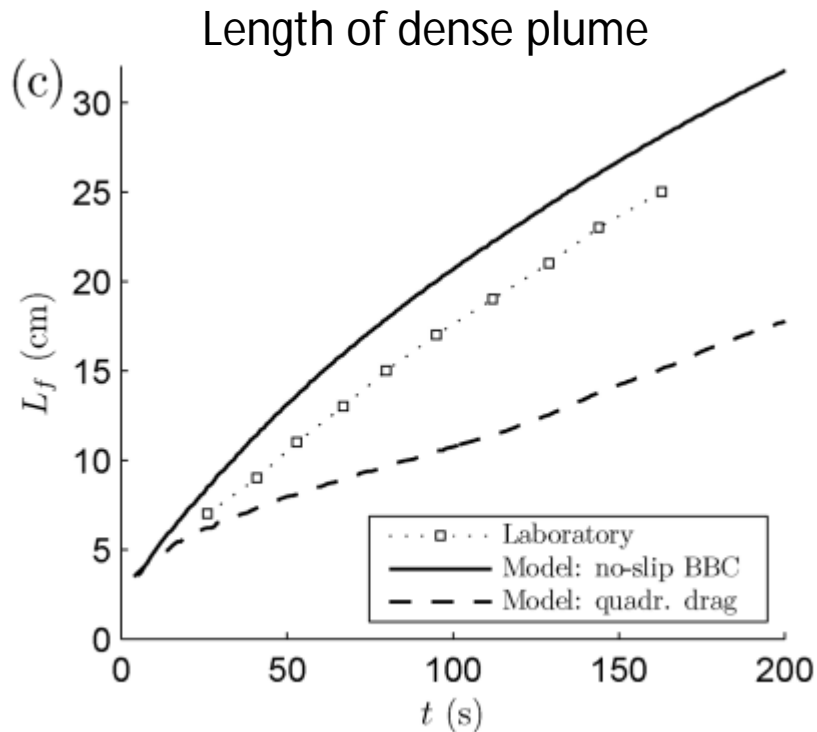
Z-coordinates, low implicit and explicit dissipation.



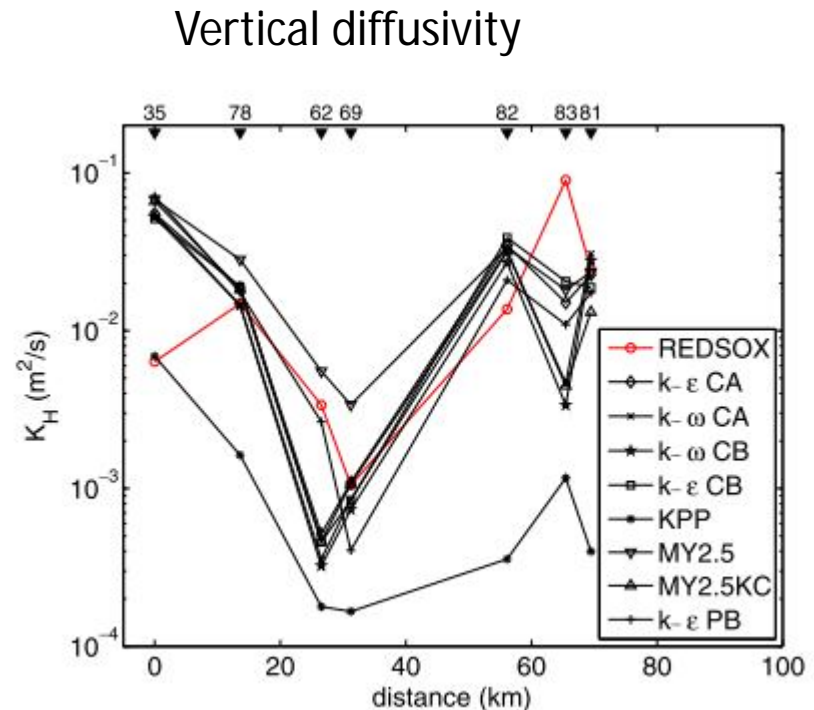
Z-coordinates, increased explicit viscosity.

To minimize spurious mixing need either isopycnal coordinates, or low grid Reynolds number (implicit or explicit) . *(Ilicak et al, 2012)*

Subgrid-scale model choices



Quadratic drag does not reproduce laboratory results in rotating laminar overflow (*Wobus et al 2011*)



2 eqn turbulence closure schemes reproduce observed diffusivities better than KPP (*Illicak et al, 2008*)

Modeling requirements for overflows

- Good resolution in frictional boundary layer – to capture Ekman drainage.
- Accurate topography, without excessive smoothing – to include small-scale channels, ridges.
- Minimal numerical mixing.
- Appropriate shear-driven mixing parameterization.